https://doi.org/10.1016/j.jclepro.2021.127745

Sustainable production of high-value gluconic acid and glucaric acid through oxidation of biomass-derived glucose: A critical review

Qiaozhi Zhang [1], Zhonghao Wan [1], Iris K.M. Yu [1, 2, #], Daniel C.W. Tsang [1, *]

[1] Department of Civil and Environmental Engineering, The Hong Kong Polytechnic University, Hung Hom, Kowloon, Hong Kong, China.

[2] Department of Chemistry and Catalysis Research Center, Technische Universität München, Lichtenbergstrasse 4, 85747 Garching, Germany.

* Corresponding author: dan.tsang@polyu.edu.hk

Co-corresponding author: iris.yu@tum.de

Abstract

Gluconic acid (GOA) and glucaric acid (GAA) are valuable chemicals for a wide range of applications, yet conventional technologies for their production suffer from low efficiency, high cost, and especially environmental concerns. It is imperative to develop sustainable heterogeneous catalytic systems exhibiting promising catalytic activity and good recyclability. In this review, base-free glucose oxidation over structure-tailored heterogeneous catalysts is discussed, and Au-based catalysts are found to present promising potential in sustainable biorefineries. To address the issue of its cost, introducing secondary metals forming bimetallic catalysts and developing non-noble metal-based catalysts are proposed as possible solutions. GAA production is of particular interest due to its high value and yet limited investigation regarding the mechanisms and system development. The feasibility of raw biomass conversion over bifunctional catalysts is also explored for the sake of industrial application. The potential of emerging technologies including ultrasound-assisted, microwave-assisted, and photocatalytic oxidation is emphasized, which allow for milder operating conditions

compared to conventional heating. This review curates the latest findings and highlights the opportunities and limitations of reported technologies, promoting the development of green catalytic systems to achieve sustainable valorization of biomass/food waste through controllable oxidation pathways.

Keywords: Glucose oxidation; platform chemicals; heterogeneous catalyst; sustainable biorefinery; waste management; biomass valorization.

Abbreviation list

Abbreviation	Full name
AC	Activated carbon
DES	Deep eutectic solvent
DFT	Density functional theory
ESR	Electron spin resonance
g-C_3N_4	Graphite-like carbon nitride
GAA	Glucaric acid
GOA	Gluconic acid
GUA	Glucuronic acid
HAP	Hydroxyapatite
HMF	5-Hydroxymethylfurfural
HPW	Phosphotungstic acid
LA	Levulinic acid
LDH	Layered double hydroxide
MPz	Metallothioporphyrazine
NHC	N-heterocyclic carbene
PVA	Polyvinylalcohol
SPR	Surface plasmon resonance
TOF	Turnover frequency
UV	Ultraviolet

Table of Contents

1. Introduction

Biomass is an abundant renewable and cleaner resource, which can be valorized to a wide range of chemicals as alternatives to fossil-derived products, alleviating the environmental impacts (*e.g.*, emission of greenhouse gases, acid rain, and $PM_{2.5}$) and easing the energy crisis. The massive amount of biomass waste remains substantially underutilized at the present stage. For instance, the residual biomass potential was estimated as 8500 PJ y^{-1} in the European Union, which exceeded the energy consumption in Italy in 2015 (Hamelin et al., 2019). This highlights the opportunity of production of value-added bio-based chemicals to achieve the Sustainable Development Goals (SDGs) proposed by United Nations (2015).

Plant-derived biomass is rich in biopolymers that comprise glucose as the monomeric unit. It can be obtained *via* hydrolysis of starch-rich food waste (Cao et al., 2018) and lignocellulosic waste (Dutta et al., 2020). Valorization of glucose is a crucial industry in biorefinery producing chemicals such as gluconic acid (GOA), glucaric acid (GAA), 5-hydroxymethylfurfural (HMF) (Yu et al., 2018), and levulinic acid (LA) (Chen et al., 2017). Among them, GOA and GAA can be utilized as additives in food, pharmaceuticals (*e.g.*, Fe, Zn, and Ca deficiency (Savas & Igor, 2007)), monomer of biodegradable polymers (*e.g.*, poly(acetonide gluconic acid) (Abtew et al., 2019) and amphiphilic polymers (Wu et al., 2016)), and green chelating agent for metal extraction/ coordination (Fischer & Bipp, 2002). Besides, GOA can serve as cement additives in construction industries (Hou & Bao, 2019), whereas GAA, a top sugar-derived building block identified by the United States Department of Energy (Werpy & Petersen, 2004), is a potential ingredient in de-icers, corrosion inhibitors (Ahuja & Singh, 2018a), and the precursor of adipic acid to substitute the conventional fossil-based feedstock (Lee et

al., 2016). The market of GAA has been forecasted to exceed US$440 million by 2024 (Ahuja & Singh, 2018a) while that of GOA will be worth US$80 million (Ahuja & Singh, 2018b).

In conventional practice, GOA and GAA can be produced by biochemical oxidation using fungi, bacteria, or enzymes (Cañete-Rodríguez et al., 2016). However, various drawbacks (*i.e.*, low productivity, vulnerability, non-recycling, wastewater production, neutralization need, *etc.*) impede their scaling-up applications. Nitric acid has been commonly used as a chemical oxidant yet the low GAA yield (< 50%) (Smith et al., 2012) and the associated environmental pollution make it less appealing for the industry. Attention has been given to developing heterogeneous catalysts that are cost-effective, recyclable, and environmentally benign to achieve sustainable biorefineries. It has been reported that GAA production using heterogeneous Pt/C catalyst induced 22% less environmental impact than nitric acid with comparable yield (Thaore et al., 2020).

Conventional heterogeneous catalysts generally comprise noble metals in monometallic (*e.g.*, Pt (Onda et al., 2008) and Pd (Liang et al., 2008)) and bimetallic (*e.g.*, AuPd (Comotti et al., 2006), AuPt (Comotti et al., 2006), PdBi (Karski et al., 2003)) forms for catalytic glucose oxidation. The effects of metal species (Comotti et al., 2006), metallic promoter (Karski et al., 2003), physicochemical properties of support (Delidovich et al., 2013), solution pH (Comotti et al., 2006), *etc.*, were examined in previous studies, in which alkali condition was necessary to achieve good catalytic performance. However, this raises environmental concerns and safety issues during operation. Most of the reported catalysts exhibited low stability and reusability.

Recent efforts have been paid to advancing heterogeneous catalysts by manoeuvring their structure-dependent catalytic activities, with a focus on high turnover frequency

(TOF) and stable performance under base-free conditions. High-resolution analytical technologies nowadays enable nano-/molecular-scale characterization, informing the control of active site formation and modification of the supports for superior catalytic activity, such as ultrasmall Au clusters supported on TiO_2 (Guo et al., 2019), Au nanoparticles supported on N-doped hierarchical porous carbon (Meng et al., 2020) and amino-functionalized mesoporous SiO_2 (Ortega-Liebana et al., 2020), and alloyed PtCu supported on TiO_2 (Shi et al., 2018). In addition, bifunctional catalysts have received significant attention to achieve the one-pot conversion of raw biomass in biorefineries. They contain acid sites that catalyze the hydrolysis of glycosidic bonds of saccharides to release glucose molecules, which are subsequently oxidized over the adjacent metal sites (Eblagon et al., 2016). To develop low-energy input protocols avoiding harsh reaction conditions, ultrasound (Amaniampong et al., 2019), microwave (Rautiainen et al., 2016), and solar energy (Zhou et al., 2017) can be employed to assist catalytic glucose oxidation *via* radical and/or thermal activation process.

While previous reviews addressed oxidation of a wide variety of biomass-derived molecules (Arias et al., 2020), focused on the use of noble metal catalysts (Cattaneo et al., 2018), or aimed at carboxylic acid production (Iglesias et al., 2020), an in-depth discussion is urgently needed for fostering the advances in glucose oxidation particularly toward high-value GOA and GAA. This review addresses the latest progress in designing heterogeneous catalysts for GOA and GAA production under eco-friendly base-free conditions. Bifunctional catalysts comprising acid and metal sites are of particular interest as they present the opportunity of direct biomass conversion to foster practical industrial application. Emerging catalytic systems assisted by ultrasound, microwave, and photocatalysis are also highlighted as cost-efficient and

energy-saving methods, and the limitations of these technologies are addressed as well. The scientific insights generated from this review are helpful for future research in devising green and promising catalytic systems for sustainable production of GOA and GAA *via* glucose oxidation.

2. Methodology

It is significant to research on clean production of GOA and GAA from biomass-derived glucose *via* catalytic oxidation. 93 publications in recent years (2015-2021) were reviewed from the Web of Science ™ Core Collection after searching for “glucose oxidation”, “gluconic acid or glucaric acid”, and “catalytic” as keywords. The citation report shows that the citations have been increasing over the past three years (**Fig. 1**). The top-record-count journals were *Catalysis Science Technology*, *Applied Catalysis B: Environmental*, *Green Chemistry*, and *ACS Sustainable Chemistry Engineering*, where the publications mostly concern the environmental issues, implying that environmentally benign process of GOA and GAA production needs to be further developed at present.

Based on the background research (**Fig. 2**), this critical review focuses on environmentally benign glucose catalytic oxidation for the production of GOA and GAA in view of their high values and research needs. A considerable number of the latest literature were critically reviewed to unveil the research progress and limitations. They were organized as follows: rationales and mechanisms (*e.g.*, reaction pathway and products, catalytic mechanisms, and catalyst deactivation), catalyst design (*e.g.*, catalysts designed for GOA/GAA production and bifunctional hydrolysis-oxidation catalysts), and emerging methods (*e.g.*, ultrasound assistance, microwave assistance,

and photocatalysis). Challenges, industrial implications, and future research directions were further identified and elaborated before conclusions.

3. Rationales and mechanisms

As the fundamental platform of this review, reaction pathway and products/by-products of catalytic glucose oxidation is firstly articulated in this section (**Fig. 3**). The purification process of GOA and GAA are then introduced considering their nature as organic acids. Catalytic mechanisms followed by the deactivation and regeneration of catalysts are elucidated for a better preparation before the subsequent sections regarding catalysts design and emerging methods.

3.1 Reaction pathway

Scheme 1 illustrates the main reaction pathway from glucose precursor to GOA and GAA products, where the aldehyde group (-CHO) on C1 of glucose is oxidized to the carboxyl group (-COOH) forming GOA. The hydroxyl group (-OH) on C6 of GOA is oxidized to -CHO and then to -COOH, forming glucuronic acid (GUA) and GAA sequentially. The yield of GAA is usually lower than GOA as the oxidation of -OH is less thermodynamically favourable than -CHO (Lee et al., 2016), and the intermediate GUA is prone to isomerization to 5-keto-GOA (Jin et al., 2016).

The side reactions include isomerization, cleavage of the C chain, and overoxidation (**Scheme 1**). Apart from the isomerization of GUA, glucose can be reversibly isomerized to fructose in base condition, which was also reported in a base-free environment in the presence of H_2O_2 that might produce OH^- (Qi et al., 2015). The C-C cleavage of hexoses and sugar acids, or the oxidization of intermediate aldehydes, produce another group of by-products, i.e., carboxylic acids with less than four carbon

atoms, including tartronic acid, glyceric acid, lactic acid, oxalic acid, glycolic acid, and formic acid (Jin et al., 2016). Arabinose (Cheng et al., 2019), glycerol (Cheng et al., 2019), and xylitol (Payormhorm et al., 2017) were also detected in photocatalytic oxidation studies. While the generation routes of the former two products were not revealed, xylitol may arise from glucose decomposition under ultraviolet (UV) irradiation. These by-products were reported in low yields, of which recovery and downstream separation may not be economically feasible. These problems suggest that science-informed catalyst structure design and functionalization are critical to suppress side reactions for selective GOA and GAA production.

3.2 Purification of products

The purification of target products is a critical process. In the conventional GOA purification process, after the addition of $Ca(OH)_2$, calcium gluconate is separated as crystal from supersaturated solution, and then stoichiometrically acidified by H_2SO_4 for Ca removal in the form of $CaSO_4$. The cation-exchange resin can also be utilized to remove Ca and obtain pure GOA (Pal et al., 2016). The environmental concerns of these purification methods should be noted, such as harsh acid conditions and wastewater discharge. An environmentally benign candidate is the membrane-based separation method, with which a continuous and recycle system can be built to supersede the conventional batch process (Banerjee et al., 2018). It was also reported that GOA can be self-precipitated without additional reagent from $FeCl_3 \cdot 6H_2O$/ethylene glycol, when using a catalytic deep eutectic solvent (DES) system (Liu et al., 2018) to achieve a clean way of production and DES recovery. As for the purification of GAA, several methods (e.g., nanofiltration and diffusion dialysis (Smith et al., 2012)) were developed to remove nitrate, which is the main residue in conventional chemical oxidation by nitric

acid. Then, mono-potassium glucarate was isolated as precipitate after base (KOH) and acid (HCl) neutralization in sequence (Smith et al., 2012). However, the use of harsh base and acid results in environmental issues; ion-exchange resins and selective sorbents have also been evaluated for the separation of GAA (Yuan et al., 2017).

3.3 Catalytic mechanisms

The catalytic mechanism of glucose oxidation is another important aspect to be further investigated. While there is limited information about GAA production in the literature, most of the mechanistic studies investigated the oxidation to GOA (*i.e.*, the first-step oxidation in **Scheme 1**), in particular, over Au-based heterogeneous catalysts. The pH value was found to be a key determinant of reaction rate, where the desorption of GOA was favoured at pH > 7 (Önal et al., 2004). The critical role of OH^- has been highlighted by using the density functional theory (DFT) method (Ishimoto et al., 2015). The OH^- in the solution phase was adsorbed on the Au surface, forming –OH for subsequent glucose adsorption. The -CHO group of glucose then interacted with OH^- in the solution phase, followed by proton transfer releasing a water molecule. The -OH adsorbed on Au surface was subsequently transferred to the intermediate forming GOA.

Although the basic solution facilitates glucose oxidation, it does not meet the requirement for sustainable development considering the environmental pollution issue. Au-based catalysts that can perform well in base-free environments have been reported for cleaner reaction, in which dissolved oxygen (Guo et al., 2019) and water (Meng et al., 2020) may participate in the oxidation. The supports could play synergistic roles in activating glucose and catalytic sites. Activated carbon (AC) was reported to facilitate the formation of secondary active sites AuO^- (Megías-Sayago et al., 2018). TiO_2 might activate the adsorbed glucose and oxygen together with Au^0 (Guo et al., 2019). Basic

sites on the hybrid composite were speculated to coordinate with the carbonyl group of glucose and facilitate hydrogen elimination for GOA production (Zhuge et al., 2019). As a non-noble metal oxide, CuO also showed the capacity to oxidize glucose without base addition (Amaniampong et al., 2015b). The corresponding mechanisms involve the dissociation of the formyl C-H bond of glucose and the insertion of the surface lattice oxygen from CuO into glucose, producing gluconate and GOA when CuO is reduced to Cu with O consumption. Such base-free conditions reduce the equipment requirement and water pollution, presenting a more economical and environmentally benign approach compared to the application of base-required catalysts.

3.4 Catalyst deactivation and regeneration

Deactivation of catalysts is commonly observed in the heterogeneous catalytic oxidation, which directly affects the reaction rate, overall conversion, and product selectivity. As for chemical deactivation, both reactant (glucose) and products (GOA and GAA) could form complexes with metals, leading to their leaching and reducing the catalytic activity (Wenkin et al., 1996). To prevent such irreversible deactivation, metals should be anchored with appropriate microstructure or nano-confinement, and/or strongly interacted with surface functionalities on the tailored support. In addition, compounds with -OH groups bound to secondary carbon atoms (*e.g.*, sugar acids and ketones) tend to be strongly adsorbed on the catalyst surface and poison the active sites (Zope & Davis, 2011). The adsorbed species could be overoxidized to by-products, decreasing the GOA and GAA selectivity. Washing the spent catalysts with NaOH solution (Abad et al., 2008) and calcination were commonly adopted to remove the adsorbed organics for catalyst regeneration, but aggressive thermal treatment might lead to thermal deactivation *via* metal sintering. Surface oxidation is another possible

deactivation pathway. It was found that Au/TiO_2 catalyst calcined in an O_2-containing environment showed low glucose conversion (< 5%) (Guo et al., 2019). The presence of Au^+ species could lead to strong interactions with the water molecules and oxygen species, blocking the active Au^0 sites from glucose and the oxidant. In contrast, another study reported that the state of Au^0 could be maintained for five runs of reaction, where the catalyst was calcinated (300 °C) in the air after each run (Meng et al., 2020). Whether surface oxidation can lead to catalyst deactivation is still debatable.

Thermal deactivation may occur as undue thermal treatment incurs metal agglomeration or sintering over the supported metal catalysts, resulting in larger particle sizes and decreased number of surface active sites. It was reported that acidic conditions accelerated Au sintering (Wang et al., 2014) and residual chloride from precursors, *e.g.*, $HAuCl_4 \cdot 3H_2O$, caused Au agglomeration during the thermal treatment (Oh et al., 2002).

3.5 Challenges

According to the above discussion of mechanisms of glucose oxidation, there are several key challenges to be investigated in depth. The detailed mechanisms of GAA production from glucose oxidation are not fully understood, although the theoretical multistep pathway has been proposed. This limits the development of solid catalysts towards high-yield and high-selectivity GAA production. The step-by-step experimental investigation combined with the DFT calculation may be needed in future studies. Another issue is the adsorbed species that poison the catalyst and lead to a series of by-products (*e.g.*, carboxylic acids) *via* overoxidation. Considering that appropriate adsorption enhances the accessibility of reactants to the active sites, it is crucial to tune the adsorption affinity and capacity by designing the structure and functionality of solid catalysts. Environmentally friendly and economically competitive purification process

of products is also worth to be investigated because the operational costs, equipment requirement, and environmental issues of present processes are still under-addressed.

4. Science-informed design of glucose oxidation catalysts

Based on the discussion regarding the rationales and mechanisms of catalytic glucose oxidation, it is noteworthy that catalyst design is one of the core issues. The advances in synthesis protocols and characterization technologies have promoted the sophisticated design of supported metallic catalysts, with a focus on developing micro-structure or hybrid composites, incorporating secondary metals and functionalized supports (**Fig. 4**). The aims are to maintain high conversion and selectivity, improve stability and reusability, and lessen the requirement of reaction conditions.

4.1 GOA production

Due to the reasonable availability and wide application, most of the previous studies took GOA as the target product from catalytic glucose oxidation. While the common approaches require alkali conditions, the oxidation of glucose to GOA in a base-free environment is more environmentally friendly and favours field-scale operation. As Au shows excellent catalytic performance compared to Pt and Pd due to its higher stability and tolerance in the acidic media, recent studies have attempted to develop innovative Au-based catalysts, in monometallic or bimetallic forms, that can facilitate base-free glucose oxidation (**Table 1**).

4.1.1 Monometallic catalysts

Monometallic catalysts are relatively simple to be prepared in comparison to bimetallic catalysts. In this section, the physicochemical properties of the catalyst supports (*i.e.*, size, species, porosity, and functional groups) followed by size and

distribution of metal particles are discussed in depth as critical determinants of catalytic performance.

Nano-size CeO_2 ($nCeO_2$) and micro-size CeO_2 (μCeO_2) were compared as supports of Au nanoparticles (Wang et al., 2014). The glucose conversion over $Au/nCeO_2$ was higher than that of $Au/\mu CeO_2$ from the second run onwards, despite similar performances in the first run. The higher reusability of $Au/nCeO_2$ can be ascribed to the abundant anchoring sites on $nCeO_2$, which could alleviate the Au leaching and hydrothermal sintering. In contrast, these issues emerged as problems for $Au/\mu CeO_2$ as Au loss and growing particle size were observed. Organic products, such as carboxylic acids and ketones, were considered as inhibitors but the catalytic activity was not recovered after NaOH wash or calcination (225 and 325 °C). It was noteworthy that a higher activity was obtained by reducing the Au loading to 0.02% on μCeO_2, which can be ascribed to the lower surface density of Au nanoparticles. As for the oxide species of support, both CeO_2 and TiO_2 showed relatively high conversion and selectivity under the selected conditions (Wang et al., 2014), while a higher Ce proportion in the support may result in a lower activity and a large proportion of Zr could favour the formation of lactic acid as a side product (Megías-Sayago et al., 2017).

Mesoporous supports can facilitate interfacial reactions and reduce metal blocking. It was reported that Au nanoparticles were confined in the mesopore channels and evenly dispersed on the surface of ordered mesoporous carbon material (CMK-3), achieving outstanding catalytic performance in the glucose oxidation among the studied catalysts (**Table 1**) (Qi et al., 2015). The catalytic activity was reduced significantly after several runs, yet it could be restored by NaOH treatment or calcination. High-temperature calcination (500 °C) however may incur metal sintering (Wang et al., 2014).

Functionalization of the supports is an emerging approach to improve catalytic performance and stability. Meng et al. (2020) synthesized a series of nitrogen-doped carbon (N-C) materials with hierarchical porous structure as the supports for Au nanoparticles, achieving excellent catalytic performance (97.62% of GOA yield, **Table 1**). The DFT results revealed that the doped N species served as the anchoring sites for Au, and pyridinic N possessed stronger binding force than graphitic N. O_2 could be adsorbed on the N atoms to enhance the charge transfer and participate in the base-free oxidation, while the nitric oxide may account for the high catalytic activity. Ortega-Liebana et al. (2020) prepared an amino-functionalized mesoporous SiO_2-supported Au-based catalyst with reference to the configuration of glucose oxidase. The catalyst exhibited good recyclability with only ~ 10% loss of activity after four runs. Glucose conversion of 85% could be obtained under mild conditions, without high temperature, pressure, and base conditions. The catalytic mechanisms are yet to be revealed.

Minerals such as hydroxyapatite (HAP) with superior ion-exchange capacity, tuneable acid and basic sites, and high stability under acid conditions are potential catalyst supports (Liu et al., 2016). By using Au/HAP catalyst, Liu et al. (2016) lowered the reaction temperature to room temperature and obtained 90.9% sodium gluconate with 0.5 equiv. Na_2CO_3 addition and catalyst deactivation was not observed after five cycles. Compared to strong alkali, Na_2CO_3 with moderate basicity was superior. Hybrid composites have been developed to capitalize on the complementary advantages of two or more support materials. Zhuge et al. (2019) prepared a complex Au/HAP-layered double hydroxide (LDH) catalyst, using CaAl-LDH with the brucite-like layer structure, high specific surface area, and abundant basic sites. The hybrid composite exhibited needle-like HAP microcrystals dispersed on the platelet-like LDH particles providing a

large surface area and facilitating strong metal-support interactions in the form of Au–O–M (M = Ca, Al). The surface basic sites were speculated to coordinate with the carbonyl group of glucose and facilitate its activation. This catalyst achieved 98.9% of glucose conversion and 99.7% of selectivity to GOA, of which the high activity was maintained for four cycles. These findings highlighted the potential of heterogeneous catalysts carrying basic sites as the sustainable alternative to alkali solutions.

Following the demonstration of controlling metal particle growth *via* support functionalization, it is necessary to determine the target particle size for cost-efficient glucose oxidation. It has been widely agreed that small particles show superior catalytic activity (Ishida et al., 2008). Guo et al. (2019) reported that Au clusters at a particle size of 1.2 nm supported on TiO_2 resulted in 92% glucose conversion with 95% GOA selectivity with high reusability for five cycles. Nevertheless, recent evidence also pointed to high-performance catalysis over relatively large particles. For the Au/C catalysts, it was identified that the optimal size was approximately 9 nm for the highest conversion with a good reusability (four runs), while the maximum TOF was achieved in the range of 15-20 nm (Megías-Sayago et al., 2018). It was also found that poor particle dispersion and a large amount of residual chlorine (from the precursor $HAuCl_4 \cdot 3H_2O$) accounted for the low catalytic activity of Au/TiO_2 catalysts (Cao et al., 2016).

4.1.2 Bimetallic catalysts

Synergistic effects of the selected metals in bimetallic catalysts offer the superiority over the monometallic catalysts. It was reported that AuPd/MgO catalyst achieved 62% glucose conversion in the air (*i.e.*, oxidant), which was higher than that for the monometallic Au/MgO and Pd/MgO catalysts (57% and 52.7%, respectively), with

100% GOA selectivity (Miedziak et al., 2014). The increase in conversion could result from alloy formation and electronic effect. However, catalyst deactivation after 24-h reaction was reported due to GOA inhibition and hydration of the support MgO to $Mg(OH)_2$, possibly leading to metal agglomeration. Cao et al. (2017) compared TiO_2-supported AuPd and AuPt catalysts and found the latter was more efficient achieving 88.9% GOA yield at 100% glucose conversion without base addition. A decrease in conversion was observed as the proportion of Au in the catalysts increased after calcination or reflux treatment, highlighting the important role of the secondary metals (Pd and Pt) in the catalysis. However, specific mechanisms were not unveiled in this study. Under the initial basic conditions, for AuPd/TiO_2-nanotube catalysts, adding 15 at% of Au into Pd led to a significant improvement of catalytic activity, though slightly lower than monometallic Au/TiO_2-nanotube catalyst (Khawaji et al., 2019). In comparison, the activity of AuPd/CeO_2-nanorod increased with the Au atomic content in AuPd and the maximum was significantly higher than that of monometallic Au and Pd catalyst, probably because Au could be negatively charged by Pd (Khawaji et al., 2020).

Similar to monometallic catalysts (**Section 4.1.1**), the properties of supports contribute to the performance of bimetallic catalysts. By comparing AuPd/TiO_2-nanotube (Khawaji et al., 2019) and AuPd/CeO_2-nanorod (Khawaji et al., 2020), it was found that the latter achieved the highest glucose conversion of 100% with 97.7% GOA selectivity due to the basicity of CeO_2 and its ability for oxygen activation. The selected catalyst maintained complete conversion (~100%) after four cycles with trivial metal leaching, which was significantly superior to the TiO_2-NT-supported counterpart.

4.2 GAA production

GAA production from glucose oxidation is one of the bottlenecks in biorefinery

because GOA shows low reactivity, which acts as an intermediate in a GAA production system (**Scheme 1**). Jin et al. (2015) prepared PtCu/TiO_2 and achieved 100% glucose conversion in the presence of base but the GAA selectivity (25.4%) was low and various by-products were generated in significant quantity. Changing the bimetals to PtPd led to a higher GAA selectivity of ~ 40% upon complete conversion (**Table 2**) because the alloyed bimetallic catalyst was effective for facilitating the GUA-to-GAA oxidative pathway rather than GUA isomerization to 5-keto-GOA (Jin et al., 2016). It was also reported that GAA yield was proportional to the atomic content of Au in bimetallic AuPd/TiO_2-NT catalyst under alkaline condition, whereas the highest GAA selectivity reached 18.5% over monometallic Au/TiO_2, with GOA being the major product at 73% glucose conversion (Khawaji et al., 2019).

Without base addition, Lee et al. (2016) obtained 74% GAA yield using commercial Pt/C catalyst, where a higher temperature, Pt loading, and pH value induced undesirable degradation of GAA to low-carbon-chain carboxylic acids and unidentified products. The alloyed AuPt/ZrO_2 catalyst prepared by Derrien et al. (2017) achieved a maximal GAA yield of 50%, which was stable for three runs and was more effective than AuPd/ZrO_2 and AuPt supported on the other materials (*e.g.*, TiO_2, CeO_2, Al_2O_3, and C). It should be noted that air was used as the oxidant in this study, which required a higher pressure (40 bar) than the use of pure O_2 (< 15 bar). Shi et al. (2018) reported that the alloyed bimetallic PtCu/TiO_2 exhibited higher selectivity to GAA compared to the monometallic Pt catalyst. This phenomenon could be attributed to (i) the change in electron density of Pt upon alloying with Cu, which affected the adsorption of glucose and products; and (ii) spatial effects of the secondary metal that might moderate C-C bond cleavage and suppress CO_2 generation as side reactions. This system required pure

421O_2 atmosphere at a relatively high pressure of 15 bar. Increasing the pressure to 30-45
422bar would result in undesirable overoxidation to CO_2. It is noteworthy that these two
423base-free systems produced GAA at the beginning of the reaction. This phenomenon is
424contrary to the observation in a base-assisted system, where the formation of GAA as a
425secondary oxidation product was not observed until the complete consumption of
426glucose (> 4-6 h), implying that glucose strongly interacted with the bimetallic surface
427and exerted an inhibitory effect (Jin et al., 2016). The cross-study comparison in this
428review suggests that such substrate inhibition might be pH-dependent, which deserves
429further investigation.

430**4.3 Bifunctional catalysts**

431 From the view of industrial application, direct utilization of raw biomass is most
432desirable in comparison to multistep conversions. To achieve this goal, bifunctional
433catalysts can be designed to produce GOA and/or GAA from di-, oligo-, or poly-
434saccharides *via* consecutive hydrolysis and oxidation. By using Au/TiO_2 catalyst, which
435showed high performance for glucose oxidation, Guo et al. (2019) converted 25% of
436cellobiose and obtained 16% selectivity towards glucose, but failed to produce GOA. In
437comparison, the bimetallic $AuPt/TiO_2$ catalyst prepared by Cao et al. (2017) converted
43873.8% cellobiose and achieved a high GOA yield of 59% in base-free condition,
439demonstrating the potential of bimetallic catalysts in facilitating raw material
440conversion. In-depth characterization of the quantity and distribution of active sites, as
441well as the mechanisms for the tandem reactions, are yet to be revealed in these
442systems. It is also of great interest to examine whether hydrolysis took place *via* an
443oxidative or acid-catalyzed pathway.

444 Based on the knowledge of solid Brønsted acids for catalyzing the hydrolysis of

445disaccharides (Xiong et al., 2018), polysaccharides (Cao et al., 2018), and raw biomass 446waste (Cao et al., 2018), incorporating acid sites on metal catalysts might enable a 447promising tandem hydrolysis-oxidation pathway. The reported bi-functional supported 448metallic catalysts (**Table 3**) had intrinsic acid sites (*e.g.*, protonated polyoxometalate) or 449acidified surfaces of the support materials. Eblagon et al. (2016) acidified mesoporous 450carbon xerogels and ordered mesoporous carbons *via* air activation. The carbon xerogel-451supported Au catalyst achieved 75% cellobiose conversion with ~ 80% GOA 452selectivity. The surface phenolic groups were proposed to facilitate cellobiose 453adsorption and acid hydrolysis. They may also protect the substrates and products from 454degradation and/or overoxidation by regulating the surface hydrophilicity and the 455adsorbed water layer. Larger pores would allow the change in conformation of 456cellobiose to make glycosidic bonds more accessible. Wan et al. (2019) unveiled 457$Cs_{2.5}H_{0.5}PW_{12}O_{40}$ as the most effective support for loading Au nanoparticles. The catalyst 458achieved 93.6% conversion of cellulose-derived levoglucosan and 93.1% GOA 459selectivity with good recyclability for five cycles, indicating its effectiveness for 460catalyzing the hydrolysis of intramolecular glycosidic linkage and the subsequent 461oxidation. These were mainly attributed to the slow hydrolysis of levoglucosan followed 462by rapid oxidation of produced glucose, thus reducing the side reactions such as 463dehydration and C-C cleavage of glucose. The generated GOA was proposed to serve as 464a Brønsted acid for autocatalytic hydrolysis. Other acidic supports, including sulfonated 465ZrO_2, phosphated TiO_2, and HZSM-5, showed a low selectivity due to the poor 466dispersion of Au particle size and/or the stronger capacity to convert GOA to by-467products.

468 Amaniampong et al. (2015a) prepared a series of TiO_2 supported Au-based bimetallic

catalysts with various secondary metals (*i.e.*, Cu, Co, Ru, and Pd). While $CoAu/TiO_2$ and $PdAu/TiO_2$ promoted the formation of fructose and glycolic acid *via* retro-aldol reaction, $RuAu/TiO_2$ and $CuAu/TiO_2$ achieved 86.9% and 88.5% GOA selectivity, respectively, at ~100% cellobiose conversion. In particular, $RuAu/TiO_2$ catalyzed the reactions over a relatively long time (9 h), as Ru-based catalysts were less selective towards GOA formation compared to other secondary metals. Because glucose was the main intermediate over this catalyst, it was speculated that cellobiose was first hydrolyzed by acid sites of support and then RuAu nanoparticles catalyzed the glucose oxidation. In comparison, it took less time (3 h) for $CuAu/TiO_2$ to achieve comparable conversion as $RuAu/TiO_2$, suggesting that Cu favoured higher activity due to the charge transfer between Cu and Au. Unlike the reaction over $RuAu/TiO_2$, cellobionic acid was the major intermediate over this catalyst, indicating that cellobiose oxidation was the first step followed by hydrolysis. It was speculated that the lattice O from the Au-CuO matrix could generate vacancies as active sites for the oxidation of glucose unit in cellobiose and adsorption sites for molecule oxygen, whereas the Lewis acid sites of TiO_2 may be responsible for the hydrolysis. It was noteworthy that both acidic and basic environments significantly lowered the selectivity of $CuAu/TiO_2$ catalyst, highlighting the potential of green catalysis in a neutral medium. The room for improvement lies in recyclability, as the GOA selectivity decreased to 70% after the fourth cycle due to the accumulation of by-products (*e.g.*, humins and carboxylic acids) on the catalyst surface.

To understand the role of lattice O, CuO nanoleaves (Amaniampong et al., 2015b) and porous structured $CuO\text{-}CeO_2$ nanospheres (Amaniampong et al., 2018) were prepared for investigation. The experimental and DFT calculation revealed that lattice O on the CuO surface could activate the formyl C-H bond of glucose and could be inserted

493into glucose for GOA formation, without consuming the dissolved O_2 and lattice O in 494CeO_2. The roles of the CeO_2 were to provide a large surface area and weaken the Cu-O 495bond for promoting the reaction. The hydrolysis-oxidation of cellobiose and cellulose to 496GOA was feasible over both CuO nanoleaves and CuO-CeO_2 (**Table 3**) yet *via* different 497routes. The hydrolytic step over CuO nanoleaves mainly relied on H_3O^+ ions generated 498in the solution phase under hydrothermal conditions, while it was catalyzed by Lewis 499acid sites localized on the catalyst surface in the case of CuO-CeO_2. These results 500underscore the potential of CuO as a non-noble metal catalyst for raw biomass 501oxidation. However, a shortcoming appears because of the irreversible consumption of 502lattice O (*i.e.*, the reduction of CuO to Cu), and activation of the spent catalyst may be 503inevitable before the next run.

504 Future research for advancing transition metal-based catalysts may refer to the 505reported homogeneous catalytic systems. Zhang et al. (2017) employed concentrated 506$FeCl_3$ solution as a bifunctional catalyst to convert cellobiose or cellulose to GOA (50-50756% yield). The authors speculated that Fe^{3+} and Cl^- ions would interact with the 508hydroxyl groups of cellulose, disrupting the inter- and intra-molecular hydrogen 509bonding and facilitating the dissolution of cellulose. It was reported that the use of 510concentrated $FeCl_3$ and DES could form a catalytic system for cellulose conversion to 511self-precipitated GOA (up to 52.7% yield) (Liu et al., 2018). Given that Fe is a low-cost 512and naturally abundant transition metal, the immobilization of active Fe species on the 513support material is economically and environmentally benign. An Ir-based 514organometallic homogeneous catalyst, denoted as [Cp*Ir(NHC)] (NHC, N-heterocyclic 515carbene), was also synthesized for the selective glucose oxidation to GOA, which could 516achieve 97% conversion and 100% selectivity in the presence of H_2SO_4 (Borja et al.,

2018). The bifunctional system was capable for starch valorization, remarkably achieving 50% GOA yield and 30% glucose yield. These findings may inform future investigations of green catalyst development in order to minimize the use of acid or base and allow for high recyclability.

4.4 Challenges

To achieve clean catalysis, Au-based heterogeneous catalysts show excellent performance and stability under base-free conditions, yet the cost of this noble metal is a challenging issue. One possible solution relies on the development of non-noble metal-based catalysts, such as Cu- and Fe-containing catalysts. Yet attention might be paid to the auto-oxidation of the reduced Cu-based catalyst and immobilization of Fe-based catalyst. Another possible solution is to develop bimetallic catalysts by introducing secondary metals. Despite the limited number of relevant studies, compelling evidences suggest the opportunity of bimetallic catalysts for base-free oxidation of glucose to GOA. In-depth characterization of the customized alloy and investigation of the activation pathways should be performed in future research. The preparation process needs to be further improved because it is often relatively complex when compared to that of monometallic catalysts. Regarding the acidic conditions for the hydrolysis, the generation of hydrated protons under hydrothermal conditions, functionalization of catalysts, and utilization of materials with intrinsic acidity are all potential alternatives.

Selective GAA production is another challenge. The investigation in this regard is insufficient at present, especially for mechanistic understanding – the prerequisite for designing efficient catalysts. The technological breakthrough can be rewarding considering the market potential of GAA. Future research is encouraged to avoid harsh

reaction conditions, such as high oxidant dosage and long reaction time, which are the major limitations of the current technologies. The relationship between substrate inhibition effect and pH value needs to be unveiled as well, which is crucial for the achievement of green production of GAA.

More sustainable glucose oxidation can be achieved by developing metal-free catalysts, considering the negative environmental impacts associated with metal leaching. It has been reported that N-doped reduced graphene oxide could act as a catalyst for glucose oxidation towards the production of organic acids with four carbon atoms or less, while the C6 acids, *i.e.*, GOA and GAA, could not be detected (Rizescu et al., 2017). These results indicated that the catalyst was capable of C-C bond cleavage in addition to glucose oxidation. It would be interesting to study whether tuning the N quantity, species, and vacancies on the metal-free carbonaceous catalysts (Wan et al., 2020) could achieve the selective oxidation of glucose to GOA or GAA.

5. Emerging oxidation methods

Apart from the structural design and functionalization of catalysts (**Section 4**), external energy input (*e.g.*, ultrasound, microwave, and solar energy) is another effective approach to enhance the efficiency of glucose oxidation. The latest research progress and their mechanisms are reviewed in the following sections as illustrated in **Fig. 5**.

5.1 Ultrasound-assisted oxidation

Ultrasound (20-2000 kHz) is a pressure wave with alternate compressions and rarefactions. Cavitation phenomenon (*i.e.*, the formation, growth, and collapse of gas microbubbles) generated by high-frequency ultrasonic irradiation (> 1000 kHz) can

result in extremely high temperature (up to 5000 K) and pressure (up to 1000 bar), which would induce chemical effects (*i.e.*, free radicals generation) and physical effects (*e.g.*, microjets, and micro-convection) (Cintas & Luche, 1999). It has been applied in several areas, such as biorefinery intensification (Martínez-Patiño et al., 2019) and wastewater treatment (Stucchi et al., 2019).

There are only a few investigations on ultrasound-assisted glucose oxidation. A sono-Fenton process was reported to yield GOA of up to 97% after low-frequency (20 kHz) ultrasonic irradiation for 15 min in the presence of $FeSO_4$ and H_2O_2, in which the generation and activity of radicals could be enhanced by ultrasound (Rinsant et al., 2014). The energy consumption could be reduced by approximately four times in this system compared with traditional heating. High-frequency (550 kHz) ultrasound was also utilized to achieve catalyst-free glucose oxidation, where sufficient radical species (*e.g.*, hydroxyl radical (·OH) and hydroperoxy radical (HO_2·)) were generated (Amaniampong et al., 2017). While GOA (40% yield) was the major product in Ar atmosphere, significant formation of GUA (94% yield) was observed in O_2 environment, mainly due to the two-step oxidation of -OH on C6 of ring-form glucose. A further study suggested the synergy between high-frequency ultrasound and CuO catalysts (Amaniampong et al., 2019). Interestingly, GUA at a maximal yield of 66% was produced under Ar atmosphere in this system, possibly due to the hydrogen radical (H·) generated under ultrasound irradiation and trapped by the surface lattice O of CuO. The reaction time ranged from 2 to 6 h for achieving the maximal yield in these high-frequency ultrasound-assisted systems, which were comparable or even superior to conventional catalytic systems in terms of power consumption (**Table 1 and 2**), demonstrating the potential in facilitating green glucose oxidation.

5.2 Microwave-assisted oxidation

Microwave is an electromagnetic wave with a frequency of 0.3-300 GHz, which could enhance high-throughput catalysis with potential energy saving (Wei et al., 2020). Its application has been demonstrated in environmental decontamination of organic pollutants, such as methyl orange (Cai et al., 2020), 2,4-dichlorophenoxy acetic acid (Sun et al., 2020), and bisphenol S (Lv et al., 2019) in wastewater. It can also assist biorefineries for value-added chemicals production, including conversion of raw biomass to LA (Cao et al., 2019), glucose isomerization to fructose (Yu et al., 2019), and dehydration of fructose to HMF (Jia et al., 2019). As for thermal effects, microwave irradiation can induce rapid volumetric heating of a microwave absorbent (*e.g.*, water) via dipolar polarization and ionic conduction, and facilitate the formation of high-temperature hotspots or micro-plasma on catalyst surface (Yu et al., 2020b). Non-thermal effects have also been proposed, in which microwave may promote the generation of free radicals (Sun et al., 2020) and/or interact with substrates and products (Yu et al., 2020c).

As shown in **Table 4**, in the presence of H_2O_2 as oxidant and Au-based catalysts, high conversion and selectivity can be achieved within a very short reaction time of 10 min, which is more favourable compared to the long reaction time (up to dozens of hours) in conventional heating (**Table 1 and 2**). Al_2O_3, CeO_2, and TiO_2 were compared as the catalyst support for microwave-assisted glucose oxidation in basic conditions (Omri et al., 2016). The Au/Al_2O_3 achieved the highest conversion (> 99%) and the highest selectivity to GOA (96%), which can be ascribed to the efficient formation of HO· and HO_2· *via* H_2O_2 decomposition on the catalyst surface. Its activity can be maintained for five cycles without significant metal leaching or changes in particle size and crystalline

phase of the support. This system was also evaluated in oxidization of other monosaccharides, disaccharides, and GOA, which generally achieved a high conversion of 71-100% in the presence of NaOH or K_2CO_3, except for methylglucoside and trehalose with zero conversion. It was noted that 31% of GAA selectivity was obtained over Au/TiO_2 despite the low glucose conversion, indicating its potential for GAA production. As the studied supports, *i.e.*, Al_2O_3, CeO_2, and TiO_2, were microwave-transparent or showed low ability in microwave absorption, it would be interesting to compare their performance with microwave-absorbing materials (*e.g.*, mesoporous carbon, biochar) to explore possible hotspot effects in future studies.

As for base-free glucose oxidation, Rautiainen et al. (2016) prepared Au/Al_2O_3 with a higher metal loading (1.8% Au) and selected a higher reaction temperature (120 °C), compared to the base-assisted system reported by Omri et al. (2016) (0.46% Au, 60 °C) (**Table 4**). The catalytic activity was stable over four cycles, despite the observed metal sintering after two runs. Metal leaching and organic adsorption were marginal. The strong capacities of aqueous glucose solution to absorb and convert microwave to thermal energy resulted in uniform and rapid heating. The Al_2O_3 support with limited microwave absorption could have prevented overheating, thus promoting the selective GOA production. Both $MgAl_2O_4$ and Al_2O_3 supports showed low rates of H_2O_2 decomposition, while a significantly higher rate could be reached after Au loading. As for non-noble metal, Khallouk et al. (2020) reported that $Zn_3V_2O_8$ could catalyze the oxidization of glucose in the presence of H_2O_2 under microwave irradiation, but the product profile was complicated including ten different acids and HMF. Neither GOA nor GAA was obtained, while the highest selectivity towards galacturonic acid resulted from GUA isomerization, which may be related to the acid site amount, hydrophilicity

of reactant, and microwave effect.

While these studies have evidenced high-performance microwave-assisted glucose oxidation, more investigations are required to reveal the microwave-involved catalytic mechanisms, especially in the presence of external oxidants. Scavenging experiments and electron spin resonance (ESR) are recommended for identifying the generation of free radicals and the DFT method can be adopted for theoretical modelling.

5.3 Photo-catalytic oxidation

Solar irradiation is a clean energy to drive photocatalysis, which attracts increasing attention due to its effectiveness, economic efficiency, low infrastructure requirement, and environmental friendliness (Chong et al., 2010). Photocatalyst (*i.e.*, semiconductor) can absorb light energy and generate electron-hole pairs *via* photoexcitation of electrons across the bandgap (*i.e.*, between the high-energy conduction band and the low-energy valence band), followed by redox reactions with the surface-adsorbed species on the catalyst. Photocatalytic wastewater treatment has proven efficacy in removing organics such as methyl orange (Yang et al., 2019), organophosphorus flame retardant (Hu et al., 2019), and antipyrine (Monteagudo et al., 2019). It has also been introduced in biorefineries for cellulose depolymerization (Zhang et al., 2018), HMF oxidation (Krivtsov et al., 2017), lignin depolymerization (Liu et al., 2020a), *etc*.

As for glucose oxidation, Colmenares et al. (2011) achieved 71.3% total selectivity to GAA, GOA, and arabitol under mild conditions (30 °C and atmospheric pressure) using TiO_2 as the photocatalyst (**Table 5**), yet the corresponding conversion was low (11.0%). It was noteworthy that acetonitrile addition could lower the affinity of reactants for TiO_2 surface to avoid overoxidation. Payormhorm et al. (2017) prepared powdered TiO_2 by using cetyltrimethylammonium bromide (CTAB, surfactant), achieving a higher glucose

661conversion of 69.5%. The problem was that the product profile was complicated, where
662arabinose and formic acid were the main products (yields above 25%) and the yields of
663GOA and xylitol were less than 10%.

664 Given the limited catalytic performance of sole TiO_2, various metal and metal oxide
665photocatalysts were prepared for more selective GOA/GAA production (**Table 5**). The
666Au/TiO_2 appeared as a potential photocatalyst because Au nanoparticle owns visible-
667light-responding characteristics, including surface plasmon resonance (SPR) effect and
668energetic/hot electrons generation under visible light (Zhou et al., 2017). In addition, Au
669nanoparticles would not induce the formation of non-selective radicals (*e.g.*, ·OH and
670singlet oxygen ($^1O_2$)) that could lead to overoxidation. The Au/TiO_2 catalyst achieved
671complete glucose conversion with 94-99% GOA selectivity under both UV and visible
672light irradiation in the presence of Na_2CO_3. It was proposed that Au nanoparticles
673enhanced the bandgap photoexcitation of TiO_2 together with the SPR effect, and the
674Na_2CO_3 addition inhibited the formation of non-selective ·OH and $^1O_2$ radicals. The
675catalyst showed relatively high reusability with unchanged selectivity and a slight
676decrease (~10%) in conversion after the fourth run.

677 With H_2O_2 addition, Omri et al. (2018) evaluated the performance of different metal
678oxides (*i.e.*, TiO_2, CeO_2, and Al_2O_3) as the support for Au nanoparticles (**Table 5**). The
679use of Au/CeO_2 achieved > 99% glucose conversion and > 95% GOA selectivity, which
680outperformed Au/TiO_2 (49% conversion, < 81% selectivity) although these two supports
681have similar bandgap values. It was speculated that CeO_2 could improve the Au
682photocatalytic ability by increasing its light absorption *via* strengthening the localized
683SPR effect and promoting charge separation in Au with a reduced recombination rate.
684The oxygen vacancies of CeO_2 favoured the Au dispersion and stability as well. For the

685oxidization of di- and oligo-saccharides, Au/CeO_2 achieved 100% conversion and >
68695% selectivity towards the corresponding primary oxidation products without
687hydrolytic cleavage, similar to a previous study (Omri et al., 2016). Despite the
688decreased TOF after five cycles, the conversion and selectivity remained high,
689indicating excellent reusability of this catalyst. The use of O_2 as the oxidant was also
690studied for Au/CeO_2-photocatalyzed glucose oxidation (Golonu et al., 2020). The
691reaction may be driven by the thermal effect induced by near-infrared radiation, instead
692of UV-promoted excitation of CeO_2 or visible photon-activated SPR effect of Au
693nanoparticles. It should be noted that alkaline (NaOH or Na_2CO_3) was employed in
694these studies (**Table 5**).

695 Several hybrid metallothioporphyrazine (MPz)-based photocatalysts were proposed
696to oxidize glucose without the use of the base, where MPzs could activate O_2 under
697visible light and show good photocatalytic activity. Cheng et al. (2019) achieved up to
69875% conversion of glucose by using ZnO/$CoPzS_8$ composite under simulated sunlight,
699but the selectivity to GOA and GAA were low (< 15%) and the main products were
700arabinose and formic acid (20-50%). Zhang et al. (2019) then used SnO_2/$FePz(SBu)_8$
701composite and accomplished 32.9% of GOA selectivity and 34.2% of glucose
702conversion at maximum. Yin et al. (2020) reported that relatively high selectivity
703(63.5% GOA and 16.9% GAA) was achieved over TiO_2/phosphotungstic acid
704(HPW)/CoPz composite, yet the glucose conversion remained low (22.2%). Recently,
705Zhang et al. (2020) prepared a graphite-like carbon nitride (g-C_3N_4)/CoPz composite,
706achieving a higher conversion of 52.1% and similar selectivity compared to those
707previously reported (Yin et al., 2020). In these studies, four active species, *i.e.*, ·OH,
708$^1O_2$, superoxide radical ($\cdot O_2^-$), and hole (h^+), were identified. It was inferred that the

decrease in ·OH formation could improve the selectivity, while $^1O_2$ and $\cdot O_2^-$, especially the former, were considered as the main active species for GOA generation. Nevertheless, the role of $^1O_2$ is debatable because it has been considered as a non-selective radical (Zhou et al., 2017). The incorporation of MPzs to the photocatalysts could promote the formation of active sites and the glucose adsorption, therefore accelerating the glucose oxidation. HPW could also facilitate the desorption of produced acids and prevent them from overoxidation. Compared to the Au-containing photocatalytic systems that required basic conditions, the MPz-based photocatalytic systems enabled the use of water only as the solvent (**Table 5**), presenting a greener practice that deserves further investigation to achieve higher glucose conversion.

5.4 Challenges

These emerging technologies, *i.e.*, ultrasound-assisted oxidation, microwave-assisted oxidation, and photocatalytic oxidation, extend the potential for the development of cleaner glucose oxidation because the catalytic reaction can be enhanced by additional or clean energy inputs mainly *via* the generation of free radical species, thus decreasing the necessity of base environment. The current progress is insufficient and several challenges are yet to be addressed. The use of ultrasound is promising as it presents the possibility of a catalyst-free system, yet the yields of several target products cannot be fine-tuned. Operational parameters should be further studied. The use of microwave is considered a high-efficiency alternative to conventional heating, but the mechanism of catalytic oxidation is not revealed, such as the roles of support material regarding its capacity of microwave absorption, which is critical for the design of functionalized catalyst. Diverse supports with varying microwave absorbability should be compared. As for photocatalytic oxidation, low yields were often obtained under the green base-

free conditions, despite the contribution of the solar-driven free radicals. Increasing the yield of the target products is the major challenge, which may be addressed by adding green oxidants and changing operating conditions. Scavenger experiments and ESR would facilitate the investigation of free radical species in the concerned reactions, as their roles in controlling the selectivity are still in debate.

Research progress has recently been made in the electrocatalytic oxidation of glucose. Various composite electrodes, such as graphene/Ni-Fe LDH (Eshghi & Kheirmand, 2017), Pd_3Cu-B/C (Chai et al., 2019), PdAu/C (Rafaïdeen et al., 2019), and Bi-Co-S (Yu et al., 2020a), were prepared to selectively oxidize glucose to GOA and GAA, together with hydrogen under some circumstances (Liu et al., 2020b). However, strong alkali solutions (NaOH and KOH) were necessary as the electrolyte in these studies. Considering the strict requirement of complex equipment setups and harsh operating conditions in the electrocatalysis, other emerging methods discussed above are considered more mature to realize the green and sustainable glucose oxidation in field applications.

6. Industrial implications and future perspectives

To achieve sustainable glucose oxidation, heterogeneous catalysts showcase a great potential in terms of good recyclability and less pollution, compared to homogeneous chemical oxidation and biochemical oxidation. Because the use of basic solutions was reported as the critical requirement over a considerable quantity of catalysts, it is more desirable to develop high-efficiency heterogeneous catalysts under base-free conditions for avoiding the issues of wastewater, corrosion, and safety. Based on the latest progress of catalyst development, Au-based catalyst is the mainstream that can meet this

requirement. Given that earth-abundant metals in homogeneous form have demonstrated catalytic activity, research could be performed to immobilize them on the support materials for high recyclability and cost reduction. Future studies may pay more attention to the rational design of catalytic systems for GAA production *via* controllable and selective secondary oxidation. From the view of industrial application, it is more applicable to tailor bifunctional catalysts for one-pot conversion of raw biomass especially for urban biomass wastes, *e.g.*, food waste and yard waste. Another potential direction is to make use of emerging oxidation methods enhanced by ultrasound, microwave, or solar energy. The mechanisms of these emerging methods are speculated to involve highly active species (hotspots and/or free radicals) resulting from electromagnetic or acoustic excitation, which should be evidenced in detail by future experimental and computational studies. To date, the economic and environmental superiorities of these emerging systems have not been fully demonstrated, considering the low conversion/selectivity and the need for bases and noble metal catalysts.

It is noteworthy that continuous reactions are preferred in the industry for mass production. The design of the catalytic reactor and process flow with proper separation and recycling should be investigated before practical scaled-up applications, where the utilization of sustainable heterogeneous catalysts and the base-free solution system highlighted in this review can simplify the catalytic conversion and wastewater treatment processes, which help reduce the environmental pollution and achieve the green and sustainable production. In addition, different from the conventional reaction, emerging methods would require additional supporting devices of energy inputs, which may need a reliable support by renewable energy sources.

7. Conclusions

Recent advances in structural design and functionalization of heterogeneous catalysts (monometallic, bimetallic, and bifunctional catalysts) and emerging energy sources (ultrasound, microwave, and solar energy) for glucose oxidation are critically reviewed. The focal points of this review capitalized on the production of GOA and GAA as the primary value-added chemicals. The key conclusions are summarized as follows.

(1) GOA and GAA are of great economic value but the conventional production processes are limited by low efficiency and environmental pollution. It is important to develop novel and clean technologies for their production *via* heterogeneous catalytic oxidation.

(2) As the addition of base is the major issue against their clean production, Au-based catalysts with science-informed design are proposed as high-efficiency and stable catalysts under the base-free conditions, yet the material cost currently limits its application. Possible solutions include developing non-noble metal-based catalysts and introducing secondary metals on Au-based catalysts. The hurdles at present are the regeneration of catalyst, immobilization of metals, and catalytic mechanisms of bimetal catalysts, which should be investigated in future research.

(3) The development of catalytic systems for GAA production is another critical issue to be addressed, considering its high value, less availability, and limited investigation compared to GOA. Future attention should be paid to the prerequisite mechanistic investigation, high-efficiency catalyst design, and solution environment adjustment.

(4) Bifunctional catalysts are preferred from the view of industrial application, in which one-pot conversion of raw biomass can be achieved *via* hydrolysis and

oxidation. The introduction of acidic sites/species into the catalytic systems can be proposed for future investigation.

(5) Emerging methods also show a great potential because the oxidation can be enhanced by the application of additional energy sources (ultrasound, microwave, and solar energy), of which detailed mechanisms and high-performance catalysts are worth to be studied.

8. Acknowledgment

The authors appreciate the financial support from the Hong Kong International Airport Environmental Fund [Phase 2] and Hong Kong Research Grants Council [PolyU 15222020].

9. References

Abad, A., Corma, A., Garcia, H. 2008. Catalyst parameters determining activity and selectivity of supported gold nanoparticles for the aerobic oxidation of alcohols: the molecular reaction mechanism. *Chemistry (Easton)*, **14**(1), 212-22.

Abtew, E., Ezra, A.F., Basu, A., Domb, A.J. 2019. Biodegradable Poly(Acetonide Gluconic Acid) for Controlled Drug Delivery. *Biomacromolecules*, **20**(8), 2934-2941.

Ahuja, K., Singh, S. 2018a. Glucaric Acid Market Size By Product (Potassium Sodium D-glucarate, Calcium D-Glucarate, D-glucaric acid-1, 4-lactone), By Application (Detergent, Food, Corrosion Inhibitors, De-Icing), Industry Analysis Report, Regional Outlook, Application Potential, Price Trend, Competitive Market Share & Forecast, 2018 – 2024. https://www.gminsights.com/industry-analysis/glucaric-acid-market.

829 Ahuja, K., Singh, S. 2018b. Gluconic Acid Market size worth over $80 mn by 2024.
830https://www.gminsights.com/pressrelease/gluconic-acid-market.

831 Amaniampong, P.N., Jia, X., Wang, B., Mushrif, S.H., Borgna, A., Yang, Y. 2015a.
832Catalytic oxidation of cellobiose over TiO2 supported gold-based bimetallic
833nanoparticles. *Catalysis Science & Technology*, **5**(4), 2393-2405.

834 Amaniampong, P.N., Karam, A., Trinh, Q.T., Xu, K., Hirao, H., Jerome, F., Chatel,
835G. 2017. Selective and Catalyst-free Oxidation of D-Glucose to D-Glucuronic acid
836induced by High-Frequency Ultrasound. *Sci Rep*, **7**, 40650.

837 Amaniampong, P.N., Trinh, Q.T., De Oliveira Vigier, K., Dao, D.Q., Tran, N.H.,
838Wang, Y., Sherburne, M.P., Jerome, F. 2019. Synergistic Effect of High-Frequency
839Ultrasound with Cupric Oxide Catalyst Resulting in a Selectivity Switch in Glucose
840Oxidation under Argon. *J Am Chem Soc*, **141**(37), 14772-14779.

841 Amaniampong, P.N., Trinh, Q.T., Li, K., Mushrif, S.H., Hao, Y., Yang, Y. 2018.
842Porous structured CuO-CeO2 nanospheres for the direct oxidation of cellobiose and
843glucose to gluconic acid. *Catal Today*, **306**, 172-182.

844 Amaniampong, P.N., Trinh, Q.T., Wang, B., Borgna, A., Yang, Y., Mushrif, S.H.
8452015b. Biomass Oxidation: Formyl C H Bond Activation by the Surface Lattice
846Oxygen of Regenerative CuO Nanoleaves. *Angew Chem Int Ed*, **54**(31), 8928-8933.

847 Arias, P.L., Cecilia, J.A., Gandarias, I., Iglesias, J., López Granados, M., Mariscal,
848R., Morales, G., Moreno-Tost, R., Maireles-Torres, P. 2020. Oxidation of
849lignocellulosic platform molecules to value-added chemicals using heterogeneous
850catalytic technologies. *Catalysis Science & Technology*, **10**(9), 2721-2757.

851 Banerjee, S., Kumar, R., Pal, P. 2018. Fermentative production of gluconic acid: A 852membrane-integrated Green process. *Journal of the Taiwan Institute of Chemical* 853*Engineers*, **84**, 76-84.

854 Borja, P., Vicent, C., Baya, M., García, H., Mata, J.A. 2018. Iridium complexes 855catalysed the selective dehydrogenation of glucose to gluconic acid in water. *Green* 856*Chem*, **20**(17), 4094-4101.

857 Cai, B., Feng, J.F., Peng, Q.Y., Zhao, H.F., Miao, Y.C., Pan, H. 2020. Super-fast 858degradation of high concentration methyl orange over bifunctional catalyst Fe/Fe3C@C 859with microwave irradiation. *J Hazard Mater*, **392**, 122279.

860 Cañete-Rodríguez, A.M., Santos-Dueñas, I.M., Jiménez-Hornero, J.E., Ehrenreich, 861A., Liebl, W., García-García, I. 2016. Gluconic acid: Properties, production methods 862and applications—An excellent opportunity for agro-industrial by-products and waste 863bio-valorization. *Process Biochem*, **51**(12), 1891-1903.

864 Cao, L., Yu, I.K.M., Cho, D.W., Wang, D., Tsang, D.C.W., Zhang, S., Ding, S., 865Wang, L., Ok, Y.S. 2019. Microwave-assisted low-temperature hydrothermal treatment 866of red seaweed (Gracilaria lemaneiformis) for production of levulinic acid and algae 867hydrochar. *Bioresour Technol*, **273**, 251-258.

868 Cao, L., Yu, I.K.M., Tsang, D.C.W., Zhang, S., Ok, Y.S., Kwon, E.E., Song, H., 869Poon, C.S. 2018. Phosphoric acid-activated wood biochar for catalytic conversion of 870starch-rich food waste into glucose and 5-hydroxymethylfurfural. *Bioresour Technol*, 871**267**, 242-248.

872 Cao, Y., Iqbal, S., Miedziak, P.J., Jones, D.R., Morgan, D.J., Liu, X., Wang, J., 873Hutchings, G.J. 2017. An investigation into bimetallic catalysts for base free oxidation 874of cellobiose and glucose. *J Chem Technol Biotechnol*, **92**(9), 2246-2253.

875 Cao, Y., Liu, X., Iqbal, S., Miedziak, P.J., Edwards, J.K., Armstrong, R.D., Morgan,
876D.J., Wang, J., Hutchings, G.J. 2016. Base-free oxidation of glucose to gluconic acid
877using supported gold catalysts. *Catalysis Science & Technology*, **6**(1), 107-117.
878 Cattaneo, S., Stucchi, M., Villa, A., Prati, L. 2018. Gold Catalysts for the Selective
879Oxidation of Biomass-Derived Products. *ChemCatChem*, **11**(1), 309-323.
880 Chai, D., Zhang, X., Chan, S.H., Li, G. 2019. Facile aqueous phase synthesis of
881Pd3Cu–B/C catalyst for enhanced glucose electrooxidation. *Journal of the Taiwan*
882*Institute of Chemical Engineers*, **95**, 139-146.
883 Chen, S.S., Yu, I.K.M., Tsang, D.C.W., Yip, A.C.K., Khan, E., Wang, L., Ok, Y.S.,
884Poon, C.S. 2017. Valorization of cellulosic food waste into levulinic acid catalyzed by
885heterogeneous Brønsted acids: Temperature and solvent effects. *Chem Eng J*, **327**, 328-
886335.
887 Cheng, M., Zhang, Q., Yang, C., Zhang, B., Deng, K. 2019. Photocatalytic oxidation
888of glucose in water to value-added chemicals by zinc oxide-supported cobalt
889thioporphyrazine. *Catalysis Science & Technology*, **9**(24), 6909-6919.
890 Chong, M.N., Jin, B., Chow, C.W.K., Saint, C. 2010. Recent developments in
891photocatalytic water treatment technology: A review. *Water Res*, **44**(10), 2997-3027.
892 Cintas, P., Luche, J.-L. 1999. The sonochemical approach. *Green Chem*, **1**(3), 115-
893125.
894 Colmenares, J.C., Magdziarz, A., Bielejewska, A. 2011. High-value chemicals
895obtained from selective photo-oxidation of glucose in the presence of nanostructured
896titanium photocatalysts. *Bioresour Technol*, **102**(24), 11254-11257.
897 Comotti, M., Pina, C.D., Rossi, M. 2006. Mono- and bimetallic catalysts for glucose
898oxidation. *J Mol Catal A: Chem*, **251**(1-2), 89-92.

899 Delidovich, I.V., Moroz, B.L., Taran, O.P., Gromov, N.V., Pyrjaev, P.A., Prosvirin,
900I.P., Bukhtiyarov, V.I., Parmon, V.N. 2013. Aerobic selective oxidation of glucose to
901gluconate catalyzed by Au/Al2O3 and Au/C: Impact of the mass-transfer processes on
902the overall kinetics. *Chem Eng J*, **223**, 921-931.

903 Derrien, E., Mounguengui-Diallo, M., Perret, N., Marion, P., Pinel, C., Besson, M.
9042017. Aerobic Oxidation of Glucose to Glucaric Acid under Alkaline-Free Conditions:
905Au-Based Bimetallic Catalysts and the Effect of Residues in a Hemicellulose
906Hydrolysate. *Ind Eng Chem Res*, **56**(45), 13175-13189.

907 Dutta, S., Yu, I.K.M., Tsang, D.C.W., Fan, J., Clark, J.H., Jiang, Z., Su, Z., Hu, C.,
908Poon, C.S. 2020. Efficient Depolymerization of Cellulosic Paper Towel Waste Using
909Organic Carbonate Solvents. *ACS Sustainable Chemistry & Engineering*, **8**(34), 13100-
91013110.

911 Eblagon, K.M., Pereira, M.F.R., Figueiredo, J.L. 2016. One-pot oxidation of
912cellobiose to gluconic acid. Unprecedented high selectivity on bifunctional gold
913catalysts over mesoporous carbon by integrated texture and surface chemistry
914optimization. *Applied Catalysis B: Environmental*, **184**, 381-396.

915 Eshghi, A., Kheirmand, M. 2017. Graphene/Ni–Fe layered double hydroxide nano
916composites as advanced electrode materials for glucose electro oxidation. *Int J*
917*Hydrogen Energy*, **42**(22), 15064-15072.

918 Fischer, K., Bipp, H.P. 2002. Removal of Heavy Metals from Soil Components and
919Soils by Natural Chelating Agents. Part II. Soil Extraction by Sugar Acids. *Water, Air,*
920*Soil Pollut*, **138**(1), 271-288.

921 Golonu, S., Pourceau, G., Quéhon, L., Wadouachi, A., Sauvage, F. 2020. Insight on 922the Contribution of Plasmons to Gold-Catalyzed Solar-Driven Selective Oxidation of 923Glucose under Oxygen. *Solar RRL*, **4**(8).

924 Guo, S., Fang, Q., Li, Z., Zhang, J., Zhang, J., Li, G. 2019. Efficient base-free direct 925oxidation of glucose to gluconic acid over TiO2-supported gold clusters. *Nanoscale*, 926**11**(3), 1326-1334.

927 Hamelin, L., Borzęcka, M., Kozak, M., Pudełko, R. 2019. A spatial approach to 928bioeconomy: Quantifying the residual biomass potential in the EU-27. *Renewable & 929Sustainable Energy Reviews*, **100**, 127-142.

930 Hou, W., Bao, J. 2019. Evaluation of cement retarding performance of cellulosic 931sugar acids. *Construction and Building Materials*, **202**, 522-527.

932 Hu, H., Zhang, H., Chen, Y., Chen, Y., Zhuang, L., Ou, H. 2019. Enhanced 933photocatalysis degradation of organophosphorus flame retardant using 934MIL-101(Fe)/persulfate: Effect of irradiation wavelength and real water matrixes. *Chem 935Eng J*, **368**, 273-284.

936 Iglesias, J., Martinez-Salazar, I., Maireles-Torres, P., Martin Alonso, D., Mariscal, R., 937Lopez Granados, M. 2020. Advances in catalytic routes for the production of carboxylic 938acids from biomass: a step forward for sustainable polymers. *Chem Soc Rev*.

939 Ishida, T., Kinoshita, N., Okatsu, H., Akita, T., Takei, T., Haruta, M. 2008. Influence 940of the support and the size of gold clusters on catalytic activity for glucose oxidation. 941*Angew Chem Int Ed Engl*, **47**(48), 9265-8.

942 Ishimoto, T., Hamatake, Y., Kazuno, H., Kishida, T., Koyama, M. 2015. Theoretical 943study of support effect of Au catalyst for glucose oxidation of alkaline fuel cell anode. 944*Appl Surf Sci*, **324**, 76-81.

945 Jia, X., Yu, I.K.M., Tsang, D.C.W., Yip, A.C.K. 2019. Functionalized zeolite-solvent 946catalytic systems for microwave-assisted dehydration of fructose to 5-947hydroxymethylfurfural. *Microporous Mesoporous Mater*, **284**, 43-52.

948 Jin, X., Zhao, M., Shen, J., Yan, W., He, L., Thapa, P.S., Ren, S., Subramaniam, B., 949Chaudhari, R.V. 2015. Exceptional performance of bimetallic Pt1Cu3/TiO2 950nanocatalysts for oxidation of gluconic acid and glucose with O2 to glucaric acid. *J* 951*Catal*, **330**, 323-329.

952 Jin, X., Zhao, M., Vora, M., Shen, J., Zeng, C., Yan, W., Thapa, P.S., Subramaniam, 953B., Chaudhari, R.V. 2016. Synergistic Effects of Bimetallic PtPd/TiO2Nanocatalysts in 954Oxidation of Glucose to Glucaric Acid: Structure Dependent Activity and Selectivity. 955*Ind Eng Chem Res*, **55**(11), 2932-2945.

956 Karski, S., Paryjczak, T., Witonñska, I. 2003. Selective oxidation of glucose to 957gluconic acid over bimetallic Pd–Me catalysts (Me= Bi, Tl, Sn, Co). *Kinet Catal*, **44**(5), 958618-622.

959 Khallouk, K., Solhy, A., Idrissi, N., Flaud, V., Kherbeche, A., Barakat, A. 2020. 960Microwave-assisted selective oxidation of sugars to carboxylic acids derivatives in 961water over zinc-vanadium mixed oxide. *Chem Eng J*, **385**.

962 Khawaji, M., Graça, I., Ware, E., Chadwick, D. 2020. Catalytic oxidation of glucose 963over highly stable AuxPdy NPs immobilised on ceria nanorods. *Catal Today*.

964 Khawaji, M., Zhang, Y., Loh, M., Graça, I., Ware, E., Chadwick, D. 2019. 965Composition dependent selectivity of bimetallic Au-Pd NPs immobilised on titanate 966nanotubes in catalytic oxidation of glucose. *Applied Catalysis B: Environmental*, **256**.

967 Krivtsov, I., García-López, E.I., Marcì, G., Palmisano, L., Amghouz, Z., García, J.R., 968Ordóñez, S., Díaz, E. 2017. Selective photocatalytic oxidation of 5-hydroxymethyl-2-

969furfural to 2,5-furandicarboxyaldehyde in aqueous suspension of g-C3N4. *Applied* 970*Catalysis B: Environmental*, **204**, 430-439.

971 Lee, J., Saha, B., Vlachos, D.G. 2016. Pt catalysts for efficient aerobic oxidation of 972glucose to glucaric acid in water. *Green Chem*, **18**(13), 3815-3822.

973 Liang, X., Liu, C.-j., Kuai, P. 2008. Selective oxidation of glucose to gluconic acid 974over argon plasma reduced Pd/Al2O3. *Green Chem*, **10**(12), 1318-1322.

975 Liu, F., Xue, Z., Zhao, X., Mou, H., He, J., Mu, T. 2018. Catalytic deep eutectic 976solvents for highly efficient conversion of cellulose to gluconic acid with gluconic acid 977self-precipitation separation. *Chem Commun*, **54**(48), 6140-6143.

978 Liu, H., Li, H., Luo, N., Wang, F. 2020a. Visible-Light-Induced Oxidative Lignin C–979C Bond Cleavage to Aldehydes Using Vanadium Catalysts. *ACS Catalysis*, **10**(1), 632-980643.

981 Liu, W.J., Xu, Z., Zhao, D., Pan, X.Q., Li, H.C., Hu, X., Fan, Z.Y., Wang, W.K., 982Zhao, G.H., Jin, S., Huber, G.W., Yu, H.Q. 2020b. Efficient electrochemical production 983of glucaric acid and H2 via glucose electrolysis. *Nature Communications*, **11**(1), 265.

984 Liu, X., Yang, Y., Su, S., Yin, D. 2016. Efficient Oxidation of Glucose into Sodium 985Gluconate Catalyzed by Hydroxyapatite Supported Au Catalyst. *Catal Lett*, **147**(2), 986383-390.

987 Lv, Y., Zhang, J., Asgodom, M.E., Liu, D., Xie, H., Qu, H. 2019. Study on the 988degradation of accumulated bisphenol S and regeneration of magnetic sludge-derived 989biochar upon microwave irritation in the presence of hydrogen peroxide for application 990in integrated process. *Bioresour Technol*, **293**, 122072.

991 Martínez-Patiño, J.C., Gullón, B., Romero, I., Ruiz, E., Brnčić, M., Žlabur, J.Š., 992Castro, E. 2019. Optimization of ultrasound-assisted extraction of biomass from olive 993trees using response surface methodology. *Ultrason Sonochem*, **51**, 487-495.

994 Megías-Sayago, C., Ivanova, S., López-Cartes, C., Centeno, M.A., Odriozola, J.A. 9952017. Gold catalysts screening in base-free aerobic oxidation of glucose to gluconic 996acid. *Catal Today*, **279**, 148-154.

997 Megías-Sayago, C., Santos, J.L., Ammari, F., Chenouf, M., Ivanova, S., Centeno, 998M.A., Odriozola, J.A. 2018. Influence of gold particle size in Au/C catalysts for base-999free oxidation of glucose. *Catal Today*, **306**, 183-190.

1000 Meng, X., Li, Z., Li, D., Huang, Y., Ma, J., Liu, C., Peng, X. 2020. Efficient base-1001free oxidation of monosaccharide into sugar acid under mild conditions using 1002hierarchical porous carbon supported gold catalysts. *Green Chem*, **22**(8), 2588-2597.

1003 Miedziak, P.J., Alshammari, H., Kondrat, S.A., Clarke, T.J., Davies, T.E., Morad, M., 1004Morgan, D.J., Willock, D.J., Knight, D.W., Taylor, S.H., Hutchings, G.J. 2014. Base-1005free glucose oxidation using air with supported gold catalysts. *Green Chem*, **16**(6), 10063132-3141.

1007 Monteagudo, J.M., Durán, A., San Martín, I., Carrillo, P. 2019. Effect of sodium 1008persulfate as electron acceptor on antipyrine degradation by solar TiO2 or TiO2/rGO 1009photocatalysis. *Chem Eng J*, **364**, 257-268.

1010 Oh, H.S., Yang, J.H., Costello, C.K., Wang, Y.M., Bare, S.R., Kung, H.H., Kung, 1011M.C. 2002. Selective Catalytic Oxidation of CO: Effect of Chloride on Supported Au 1012Catalysts. *J Catal*, **210**(2), 375-386.

1013 Omri, M., Pourceau, G., Becuwe, M., Wadouachi, A. 2016. Improvement of Gold-
1014Catalyzed Oxidation of Free Carbohydrates to Corresponding Aldonates Using
1015Microwaves. *ACS Sustainable Chemistry & Engineering*, **4**(4), 2432-2438.
1016 Omri, M., Sauvage, F., Busby, Y., Becuwe, M., Pourceau, G., Wadouachi, A. 2018.
1017Gold Catalysis and Photoactivation: A Fast and Selective Procedure for the Oxidation of
1018Free Sugars. *ACS Catalysis*, **8**(3), 1635-1639.
1019 Önal, Y., Schimpf, S., Claus, P. 2004. Structure sensitivity and kinetics of D-glucose
1020oxidation to D-gluconic acid over carbon-supported gold catalysts. *J Catal*, **223**(1), 122-
1021133.
1022 Onda, A., Ochi, T., Kajiyoshi, K., Yanagisawa, K. 2008. A new chemical process for
1023catalytic conversion of d-glucose into lactic acid and gluconic acid. *Applied Catalysis*
1024*A: General*, **343**(1-2), 49-54.
1025 Ortega-Liebana, M.C., Bonet-Aleta, J., Hueso, J.L., Santamaria, J. 2020. Gold-Based
1026Nanoparticles on Amino-Functionalized Mesoporous Silica Supports as Nanozymes for
1027Glucose Oxidation. *Catalysts*, **10**(3).
1028 Pal, P., Kumar, R., Banerjee, S. 2016. Manufacture of gluconic acid: A review
1029towards process intensification for green production. *Chemical Engineering and*
1030*Processing: Process Intensification*, **104**, 160-171.
1031 Payormhorm, J., Chuangchote, S., Kiatkittipong, K., Chiarakorn, S., Laosiripojana,
1032N. 2017. Xylitol and gluconic acid productions via photocatalytic-glucose conversion
1033using TiO 2 fabricated by surfactant-assisted techniques: Effects of structural and
1034textural properties. *Mater Chem Phys*, **196**, 29-36.

1035 Qi, P., Chen, S., Chen, J., Zheng, J., Zheng, X., Yuan, Y. 2015. Catalysis and
1036Reactivation of Ordered Mesoporous Carbon-Supported Gold Nanoparticles for the
1037Base-Free Oxidation of Glucose to Gluconic Acid. *ACS Catalysis*, **5**(4), 2659-2670.
1038 Rafaïdeen, T., Baranton, S., Coutanceau, C. 2019. Highly efficient and selective
1039electrooxidation of glucose and xylose in alkaline medium at carbon supported alloyed
1040PdAu nanocatalysts. *Applied Catalysis B: Environmental*, **243**, 641-656.
1041 Rautiainen, S., Lehtinen, P., Vehkamäki, M., Niemelä, K., Kemell, M., Heikkilä, M.,
1042Repo, T. 2016. Microwave-assisted base-free oxidation of glucose on gold nanoparticle
1043catalysts. *Catal Commun*, **74**, 115-118.
1044 Rinsant, D., Chatel, G., Jérôme, F. 2014. Efficient and Selective Oxidation of D-
1045Glucose into Gluconic acid under Low-Frequency Ultrasonic Irradiation.
1046*ChemCatChem*, **6**(12), 3355-3359.
1047 Rizescu, C., Podolean, I., Albero, J., Parvulescu, V.I., Coman, S.M., Bucur, C.,
1048Puche, M., Garcia, H. 2017. N-Doped graphene as a metal-free catalyst for glucose
1049oxidation to succinic acid. *Green Chem*, **19**(8), 1999-2005.
1050 Savas, A., Igor, G.M. 2007. Gluconic Acid Production. *Recent Patents on*
1051*Biotechnology*, **1**(2), 167-180.
1052 Shi, H., Thapa, P.S., Subramaniam, B., Chaudhari, R.V. 2018. Oxidation of Glucose
1053Using Mono- and Bimetallic Catalysts under Base-Free Conditions. *Organic Process*
1054*Research & Development*, **22**(12), 1653-1662.
1055 Smith, T.N., Hash, K., Davey, C.L., Mills, H., Williams, H., Kiely, D.E. 2012.
1056Modifications in the nitric acid oxidation of D-glucose. *Carbohydr Res*, **350**, 6-13.

1057 Stucchi, M., Cerrato, G., Bianchi, C.L. 2019. Ultrasound to improve both synthesis
1058and pollutants degradation based on metal nanoparticles supported on TiO2. *Ultrason*
1059*Sonochem*, **51**, 462-468.

1060 Sun, Y., Yu, I.K.M., Tsang, D.C.W., Fan, J., Clark, J.H., Luo, G., Zhang, S., Khan,
1061E., Graham, N.J.D. 2020. Tailored design of graphitic biochar for high-efficiency and
1062chemical-free microwave-assisted removal of refractory organic contaminants. *Chem*
1063*Eng J*, **398**, 125505.

1064 Thaore, V.B., Armstrong, R.D., Hutchings, G.J., Knight, D.W., Chadwick, D., Shah,
1065N. 2020. Sustainable production of glucaric acid from corn stover via glucose oxidation:
1066An assessment of homogeneous and heterogeneous catalytic oxidation production
1067routes. *Chem Eng Res Des*, **153**, 337-349.

1068 United Nations Development Programme. 2015. The Sustainable Development
1069Goals. https://www.undp.org/content/undp/en/home/copyright-and-termsofuse.html.

1070 Wan, Y., Zhang, L., Chen, Y., Lin, J., Hu, W., Wang, S., Lin, J., Wan, S., Wang, Y.
10712019. One-pot synthesis of gluconic acid from biomass-derived levoglucosan using a
1072Au/Cs2.5H0.5PW12O40 catalyst. *Green Chem*, **21**(23), 6318-6325.

1073 Wan, Z., Xu, Z., Sun, Y., He, M., Hou, D., Cao, X., Tsang, D.C.W. 2021. Critical
1074impact of nitrogen vacancies in nonradical carbocatalysis on nitrogen-doped graphitic
1075biochar. *Environ. Sci. Technol.*, in press.

1076 Wang, Y., Van de Vyver, S., Sharma, K.K., Román-Leshkov, Y. 2014. Insights into
1077the stability of gold nanoparticles supported on metal oxides for the base-free oxidation
1078of glucose to gluconic acid. *Green Chem*, **16**(2), 719-726.

1079 Wei, R., Wang, P., Zhang, G., Wang, N., Zheng, T. 2020. Microwave-responsive
1080catalysts for wastewater treatment: A review. *Chem Eng J*, **382**, 122781.

1081 Wenkin, M., Touillaux, R., Ruiz, P., Delmon, B., Devillers, M. 1996. Influence of
1082metallic precursors on the properties of carbon-supported bismuth-promoted palladium
1083catalysts for the selective oxidation of glucose to gluconic acid. *Applied Catalysis A:*
1084*General*, **148**(1), 181-199.

1085 Werpy, T., Petersen, G. 2004. Top value added chemicals from biomass: volume I--
1086results of screening for potential candidates from sugars and synthesis gas. National
1087Renewable Energy Lab., Golden, CO (US).

1088 Wu, Y., Enomoto-Rogers, Y., Masaki, H., Iwata, T. 2016. Synthesis of Crystalline
1089and Amphiphilic Polymers from d-Glucaric Acid. *ACS Sustainable Chemistry &*
1090*Engineering*, **4**(7), 3812-3819.

1091 Xiong, X., Yu, I.K.M., Chen, S.S., Tsang, D.C.W., Cao, L., Song, H., Kwon, E.E.,
1092Ok, Y.S., Zhang, S., Poon, C.S. 2018. Sulfonated biochar as acid catalyst for sugar
1093hydrolysis and dehydration. *Catal Today*, **314**, 52-61.

1094 Yang, J., Du, J., Li, X., Liu, Y., Jiang, C., Qi, W., Zhang, K., Gong, C., Li, R., Luo,
1095M. 2019. Highly hydrophilic TiO2 nanotubes network by alkaline hydrothermal method
1096for photocatalysis degradation of methyl orange. *Nanomaterials*, **9**(4), 526.

1097 Yin, J., Zhang, Q., Yang, C., Zhang, B., Deng, K. 2020. Highly selective oxidation of
1098glucose to gluconic acid and glucaric acid in water catalyzed by an efficient synergistic
1099photocatalytic system. *Catalysis Science & Technology*, **10**(7), 2231-2241.

1100 Yu, B., Liu, Y., Miao, Y. 2020a. Nanorods of Bi–Co–S for Electrocatalysis of
1101Glucose Oxidation and Hydrogen Evolution. *Journal of Electrochemical Energy*
1102*Conversion and Storage*, **17**(3).

1103 Yu, I.K.M., Chen, H., Abeln, F., Auta, H., Fan, J., Budarin, V.L., Clark, J.H.,
1104Parsons, S., Chuck, C.J., Zhang, S., Luo, G., Tsang, D.C.W. 2020b. Chemicals from

lignocellulosic biomass: A critical comparison between biochemical, microwave and thermochemical conversion methods. *Crit Rev Environ Sci Technol*, 1-54.

Yu, I.K.M., Fan, J., Budarin, V.L., Bouxin, F.P., Clark, J.H., Tsang, D.C.W. 2020c. Evidences of starch–microwave interactions under hydrolytic and pyrolytic conditions. *Green Chem*, **22**(20), 7109-7118.

Yu, I.K.M., Tsang, D.C.W., Yip, A.C.K., Hunt, A.J., Sherwood, J., Shang, J., Song, H., Ok, Y.S., Poon, C.S. 2018. Propylene carbonate and γ-valerolactone as green solvents enhance Sn(iv)-catalysed hydroxymethylfurfural (HMF) production from bread waste. *Green Chem*, **20**(9), 2064-2074.

Yu, I.K.M., Xiong, X., Tsang, D.C.W., Ng, Y.H., Clark, J.H., Fan, J., Zhang, S., Hu, C., Ok, Y.S. 2019. Graphite oxide- and graphene oxide-supported catalysts for microwave-assisted glucose isomerisation in water. *Green Chem*, **21**(16), 4341-4353.

Yuan, W., Ding, R.-H., Ge, H., Zhu, P.-L., Ma, S.-S., Zhang, B., Song, X.-M. 2017. Solid-phase extraction of d -glucaric acid from aqueous solution. *Sep Purif Technol*, **175**, 352-357.

Zhang, B., Li, J., Guo, L., Chen, Z., Li, C. 2018. Photothermally promoted cleavage of β-1,4-glycosidic bonds of cellulosic biomass on Ir/HY catalyst under mild conditions. *Applied Catalysis B: Environmental*, **237**, 660-664.

Zhang, H., Li, N., Pan, X., Wu, S., Xie, J. 2017. Direct Transformation of Cellulose to Gluconic Acid in a Concentrated Iron(III) Chloride Solution under Mild Conditions. *ACS Sustainable Chemistry & Engineering*, **5**(5), 4066-4072.

Zhang, Q., Ge, Y., Yang, C., Zhang, B., Deng, K. 2019. Enhanced photocatalytic performance for oxidation of glucose to value-added organic acids in water using iron thioporphyrazine modified SnO2. *Green Chem*, **21**(18), 5019-5029.

1129 Zhang, Q., Xiang, X., Ge, Y., Yang, C., Zhang, B., Deng, K. 2020. Selectivity
1130enhancement in the g-C3N4-catalyzed conversion of glucose to gluconic acid and
1131glucaric acid by modification of cobalt thioporphyrazine. *J Catal*, **388**, 11-19.
1132 Zhou, B., Song, J., Zhang, Z., Jiang, Z., Zhang, P., Han, B. 2017. Highly selective
1133photocatalytic oxidation of biomass-derived chemicals to carboxyl compounds over Au/
1134TiO2. *Green Chem*, **19**(4), 1075-1081.
1135 Zhuge, Y., Fan, G., Lin, Y., Yang, L., Li, F. 2019. A hybrid composite of
1136hydroxyapatite and Ca-Al layered double hydroxide supported Au nanoparticles for
1137highly efficient base-free aerobic oxidation of glucose. *Dalton Trans*, **48**(25), 9161-
11389172.
1139 Zope, B.N., Davis, R.J. 2011. Inhibition of gold and platinum catalysts by reactive
1140intermediates produced in the selective oxidation of alcohols in liquid water. *Green*
1141*Chem*, **13**(12).

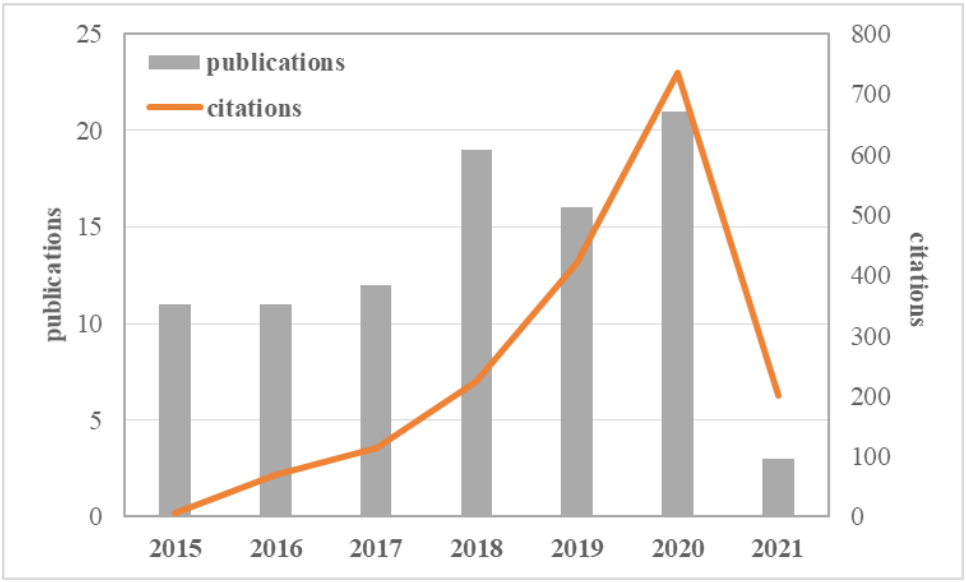

Fig. 1 Times cited and publications over time based on citation report from Web of Science ™ database

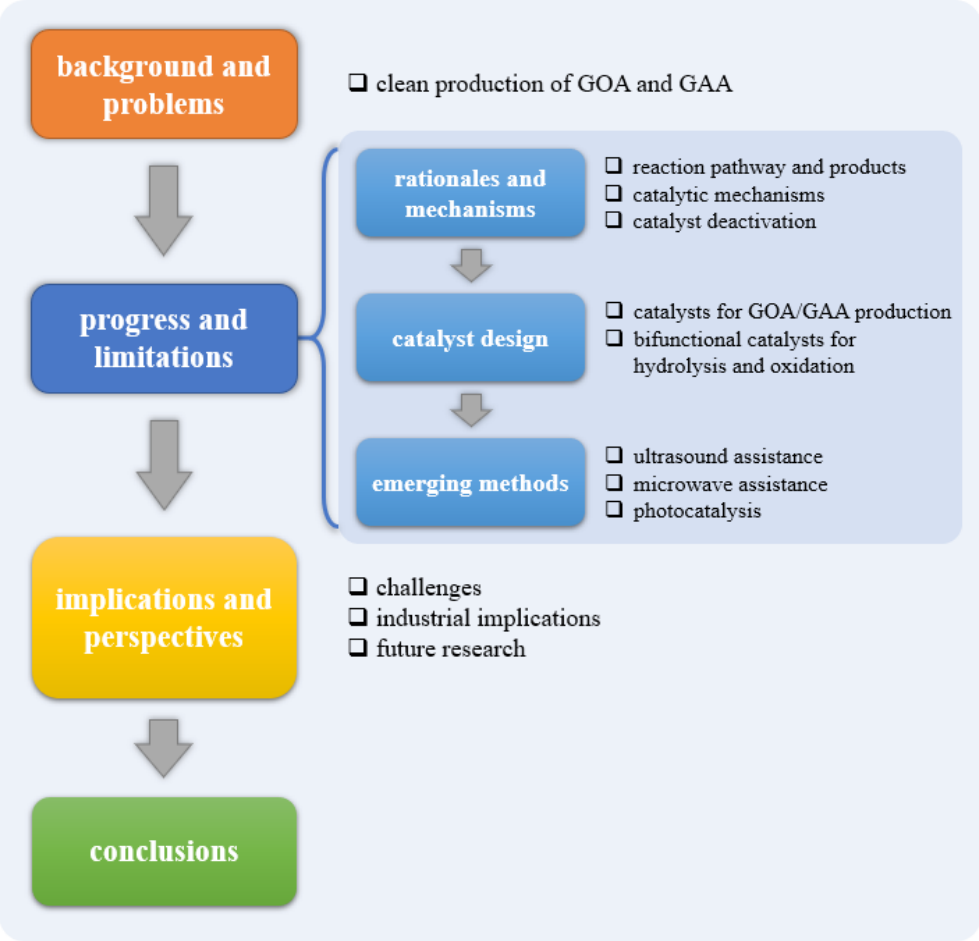

Fig. 2 Flow chart of the outline of this literature review

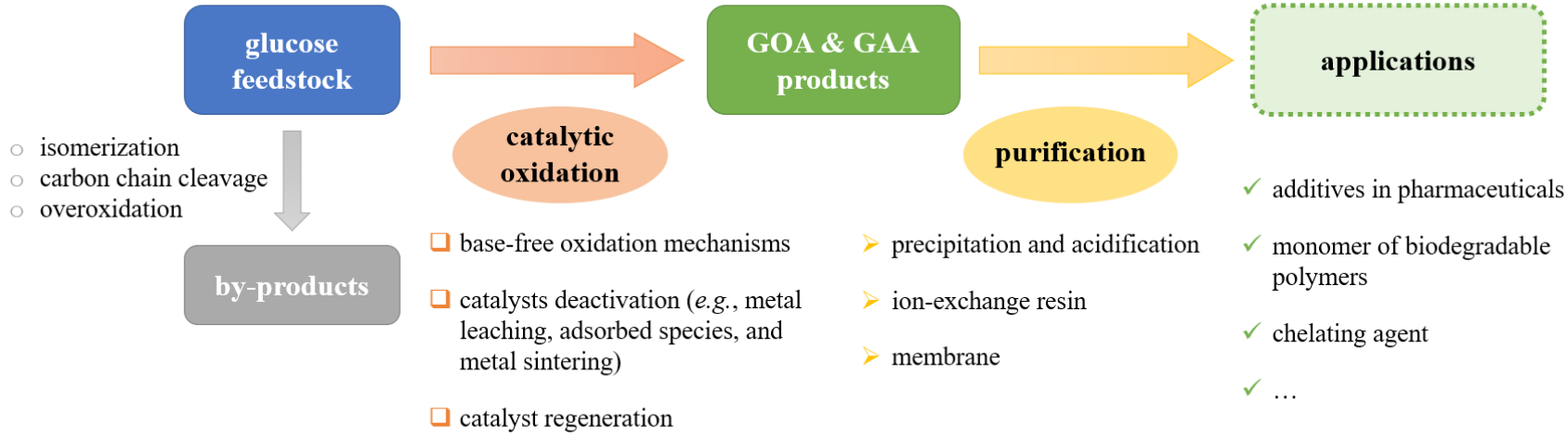

Fig. 3 Main contents of Section 3 regarding the rationales and mechanisms of catalytic glucose oxidation

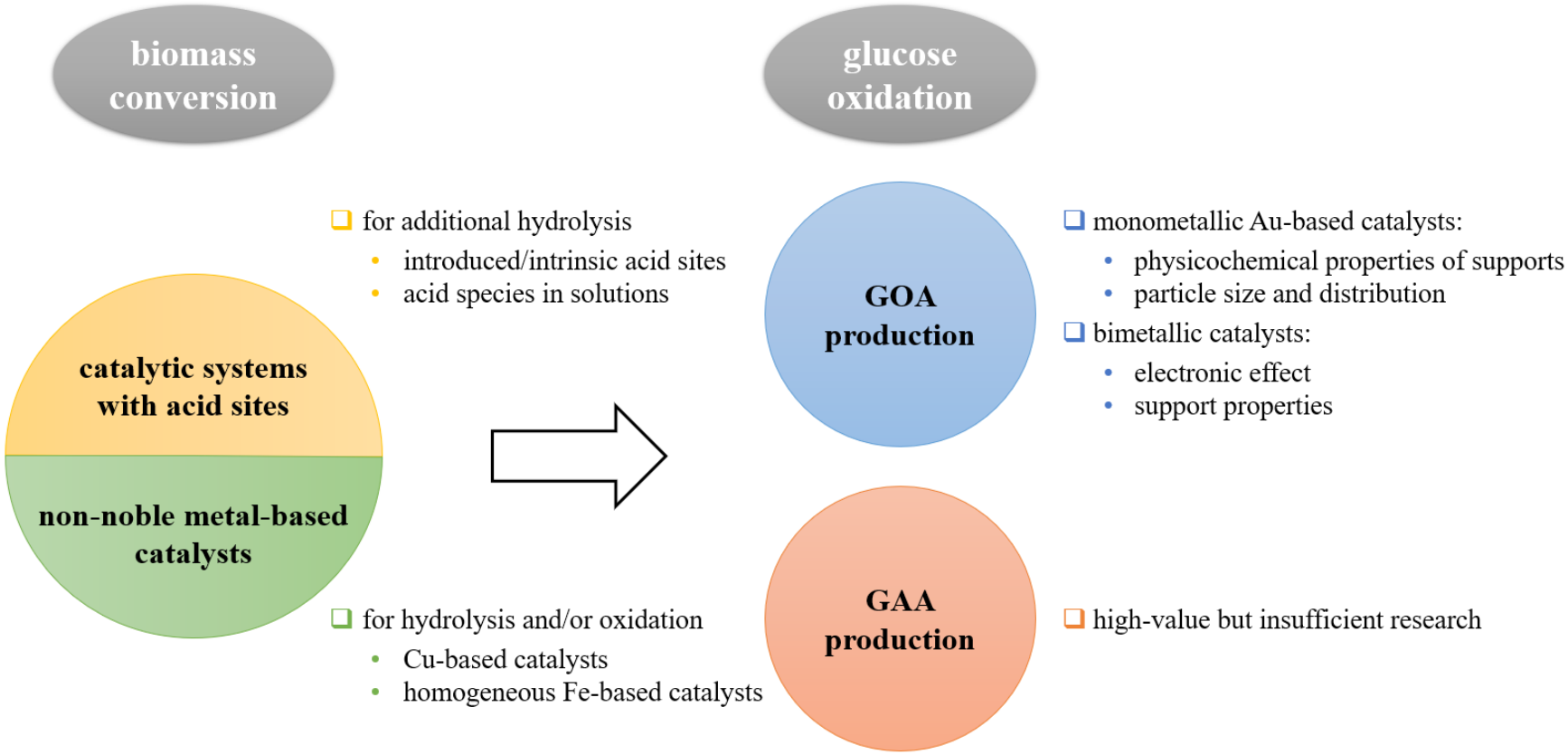

Fig. 4 Main contents of Section 4 regarding the catalyst design for biomass-derived glucose oxidation

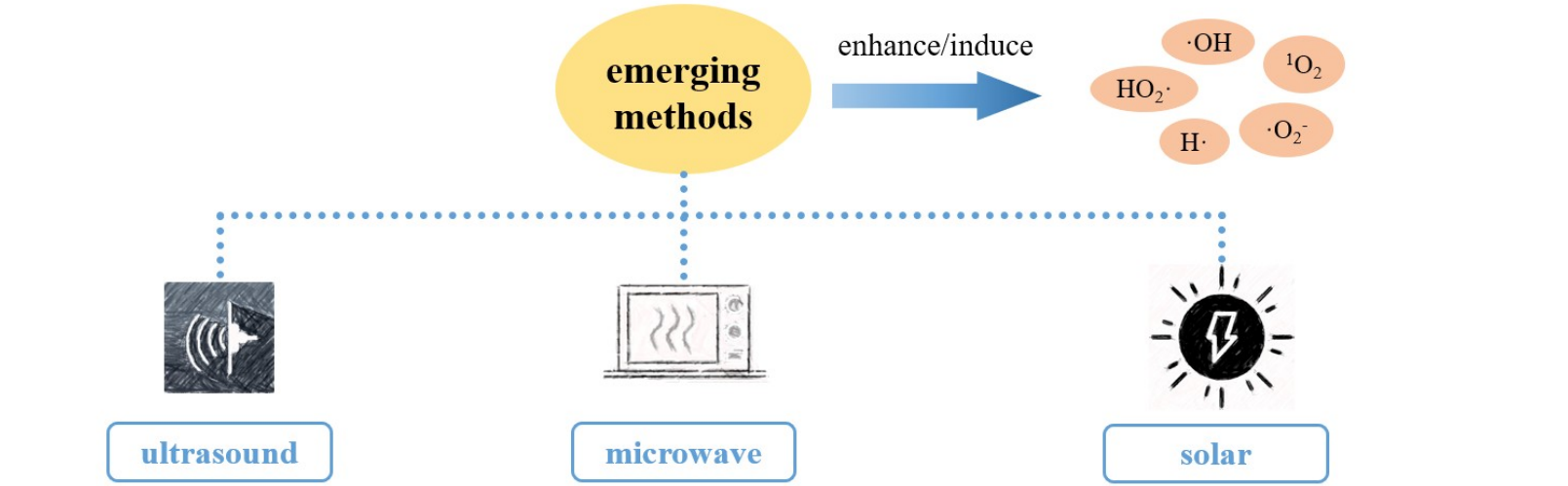

1155

1156 Fig. 5 Main contents in Section 5 regarding the emerging oxidation methods

1157

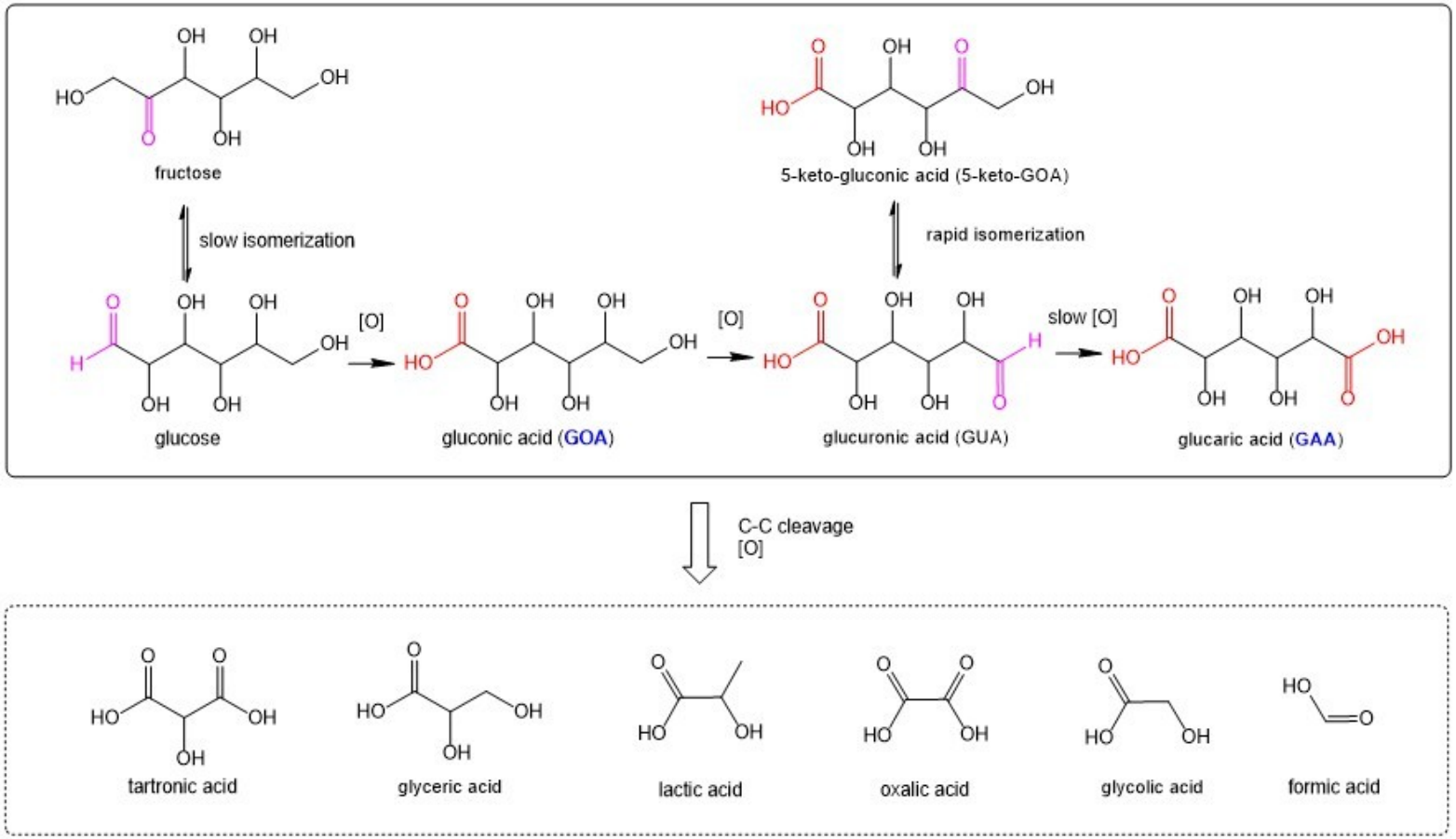

Scheme 1 Plausible reaction pathway of glucose oxidation and detected by-products (redrawn based on references) (Jin et al., 2016; Lee et al., 2016)

Table 1 GOA production under base-free glucose oxidation

entry	Operating conditions							Catalytic efficiency				Ref.
	Catalyst [a] and dosage	Initial glucose concentration/mol L^{-1}	Molar ratio of glucose to loading metal	Oxidant and dosage	Temperature /°C	Time/ h	pH	TOF/s^{-1}	Conversion/%	Selectivity/%	Yield/ %	
1	0.5%Au/nCeO_2, NA	0.167	140	O_2, $p(O_2)$=2.3 bar	65	2	NC	—	74	95	70.3 *	(Wang et al., 2014)
2	0.6%Au/μCeO_2, —	0.167	140	O_2, $p(O_2)$=2.3 bar	65	2	NC	—	76	96	73.0 *	(Wang et al., 2014)
3	0.94%Au/CMK-3, 1.98 mg mL^{-1}	0.1	1000	O_2, $p(O_2)$=0.3 MPa	110	2	NC	4.92 [g]	92.4	87.5	80.9 *	(Qi et al., 2015)
4	0.97%Au/N-C-3, 1.67 mg mL^{-1}	0.037	437	O_2, $p(O_2)$=2 bar	100	2	NC	—	98.76	98.8 *	97.62	(Meng et al., 2020)
5	1%Au/MCM41-NH_2, 0.025 mg mL^{-1}	0.15	—	dissolved O_2, 6–8 mg/L	37	0.75	7.4 [e]	—	85	100	85.0 *	(Ortega-Liebana et al., 2020)
6	1.57%Au/HAP, 4 mg mL^{-1}	0.15	—	O_2, 30 mL min^{-1}	Room temperature	1	NC [f]	1.24	100	90.9	90.9	(Liu et al., 2016)
7	0.2%Au/HAP-LDH, —	0.167	1000	O_2, $p(O_2)$=0.5 MPa	110	2	NC	5.62	98.9	99.7	98.6 *	(Zhuge et al., 2019)
8	0.5%Au/TiO_2 [b], 3.6 mg mL^{-1}	0.1	—	O_2, $p(O_2)$=1 MPa	110	2	NC	0.53 [h]	92	95	87.4 *	(Guo et al., 2019)
9	2%Au/AC [c], —	0.2	100	O_2, $p(O_2)$=0.1 MPa	40	18	NC	(4 ~ 15)×10^{-3}	70 ~ 80	100	70 ~ 80 *	(Megías-Sayago et al., 2018)
10	1%Au1%Pt/TiO_2, 2.5 mg g^{-1}	0.056	—	O_2, $P(O_2)$=3 bar	160	1	NC	0.030	100	88.9 *	88.9	(Cao et al., 2017)
11	0.5%AuPd/MgO [d], 12 mg mL^{-1}	0.5	—	air, atmosphere	50	24	NC	—	62	100	62 *	(Miedziak et al., 2014)

1163a: metal loading is weight ratio; b: reduced by 5 v% hydrogen gas at 150 °C; c: Au particle size range of 4 ~ 23 nm; d: heat-treated sequentially by air and nitrogen; e:
1164maintained by sodium acetate/acetic acid buffer solution; f: 0.075 mol L^{-1} Na_2CO_3 added initially, and product was sodium gluconate; g: calculated by the conversion at
11655 min; h: calculated by the conversion at 15 min

1166TOF: turnover frequency; HAP: hydroxyapatite; LDH: layered double hydroxide; AC: activated carbon; NC: not controlled; — : not available or not applicable; *
1167calculated based on equation: yield (%) = conversion (%) × selectivity (%) /100
1168

1169 Table 2 Selected GAA production from glucose catalytic oxidation

entry	Operating conditions							Catalytic efficiency				Ref.
	Catalyst [a] and dosage	Initial glucose concentration/mol L^{-1}	Molar ratio of glucose to loading metal	Oxidant and dosage	Temperature/°C	Time/h	pH and reagent	TOF/s^{-1}	Conversion/%	Selectivity/%	Yield/%	
1	1%Pt1%Pd/TiO_2, 2 mg mL^{-1}	0.167	—	O_2, 60 mL min^{-1}	45	24	11.5 [b], NaOH	0.668	100	41.2	41.2 *	(Jin et al., 2016)
2	5%Pt/C, 40 mg mL^{-1}	0.555	54	O_2, $p(O_2)$=13.8 bar	80	10	NC	—	99	74	74	(Lee et al., 2016)
3	3.5%Au3.45%Pt/ZrO_2, —	0.25	80	air, p(air)=40 bar	100	4	NC	0.984	100	50 *	50	(Derrien et al., 2017)
4	4.13%Pt1.70%Cu/TiO2, 20 mg mL^{-1}	0.278	—	O_2, $p(O_2)$=15 bar	90	12	NC	—	92	60	55.2 *	(Shi et al., 2018)

1170a: metal loading is weight ratio; b: initial pH and not controlled during reaction

1171TOF: turnover frequency; NC: not controlled; — : not available or not applicable; * calculated based on equation: yield (%) = conversion (%) × selectivity (%) /100

1172

1173 Table 3 Oxidation of disaccharides and polysaccharides

entry	Operating conditions						Catalytic efficiency					Ref.
	Catalyst [a] and dosage	Raw material and loading	Oxidant and dosage	Temperature/°C	Time/h	pH and reagent	Conversion/%	Selectivity/%		Yield/%		
								GOA	glucose	GOA	glucose	
1	1%Au-1%Pt/TiO_2, 2.5 mg g^{-1}	Cellobiose, 10 mg g^{-1}	O_2, $P(O_2)$=3 bar	150	3	NC	73.8	80.0 *	—	59.0	—	(Cao et al., 2017)
2	1%Au/CX [b], 2 mg mL^{-1}	Cellobiose, 12 mmol L^{-1}	O_2, $P(O_2)$=5 bar	145	1.25	NC	~ 75	79.8	—	~ 60	—	(Eblagon et al., 2016)
3	0.96%Au/$Cs_{2.5}H_{0.5}PW_{12}O_{40}$, 7.5 mg mL^{-1}	Levoglucosan, 12.5 mg mL^{-1}	O_2, $P(O_2)$=0.5 MPa	145	3	NC	93.6	93.1	0	87.1	0 *	(Wan et al., 2019)
4	0.94%Au/nano-ZrO_2-SO_4^{2-}, 7.5 mg mL^{-1}	Levoglucosan, 12.5 mg mL^{-1}	O_2, $P(O_2)$=0.5 MPa	145	3	NC	94.6	31.2	9.4	29.5 *	8.9 *	(Wan et al., 2019)
5	0.95%Au/TiO_2-PO_4^{3-}, 7.5 mg mL^{-1}	Levoglucosan, 12.5 mg mL^{-1}	O_2, $P(O_2)$=0.5 MPa	145	3	NC	99.5	46.8	12.4	46.6 *	12.3 *	(Wan et al., 2019)
6	1.0%Au/HZSM-5 7.5 mg mL^{-1}	Levoglucosan, 12.5 mg mL^{-1}	O_2, $P(O_2)$=0.5 MPa	145	3	NC	41.1	25.0	71.5	10.3 *	29.4 *	(Wan et al., 2019)
7	0.5%Cu0.5%Au/TiO_2, 5 mg mL^{-1}	Cellobiose, 0.03 mmol mL^{-1}	O_2, $P(O_2)$=1 MPa	145	3	NC	100	88.5	11.5	88.5 *	11.5 *	(Amaniampong et al., 2015a)
8	CuO [c] nanoleaves, 2.5 mg mL^{-1}	Cellobiose, 0.03 mmol mL^{-1}	— [e]	200	0.5	NC	100	71.7 *	—	71.7	—	(Amaniampong et al., 2015b)
9	CuO nanoleaves, —	Cellulose, —	— [e]	200	3	NC	96.8	61.0 *	—	59.0	—	(Amaniampong et al., 2015b)
10	CuO-CeO_2 [d] nanospheres, 25 wt%	Cellobiose, 13.7 mg mL^{-1}	— [e]	160	3	NC	68	~ 5.0 *	—	~ 51	—	(Amaniampong et al., 2018)

1174a: metal loading is weight ratio; b: CX (carbon xerogel) prepared with pH=5.6 and activated by air (O_2), and Au/CX reduced by modified citric method; c: after one
1175reaction cycle, regenerated by reoxidation under oxygen flow; d: molar ratio = 1:1; e: purged with N_2

1176TOF: turnover frequency; NC: not controlled; — : not available or not applicable; * calculated based on equation: yield (%) = conversion (%) × selectivity (%) /100
1177

1178 Table 4 Microwave-assisted catalytic oxidation of glucose

entry	Operating conditions							Catalytic efficiency				Ref.
	Catalyst [a] and dosage	Initial glucose concentration/mg mL^{-1}	Molar ratio of glucose to loading metal	Oxidant and dosage	Temperature/°C	Time/min	pH and reagent	TOF/h^{-1}	Conversion/%	Selectivity [d]/%	yield [e, *]/%	
1	0.46%Au/Al_2O_3 [b], 0.5 mg mL^{-1}	50	—	H_2O_2, 3 equiv.	60	10	— [c], NaOH	312000	> 99	96	95.0	(Omri et al., 2016)
2	0.54%Au/CeO_2 [b], 0.5 mg mL^{-1}	50	—	H_2O_2, 3 equiv.	60	10	— [c], NaOH	438000	92	93	85.6	(Omri et al., 2016)
3	0.73%Au/TiO_2 [b], 0.5 mg mL^{-1}	50	—	H_2O_2, 3 equiv.	60	10	— [c], NaOH	75000	46	69	31.7	(Omri et al., 2016)
4	2.3%$Au/MgAl_2O_4$, 1.2 mg mL^{-1}	22	870	H_2O_2, 2.2 equiv.	120	10	NC	10400	54	93	50.2	(Rautiainen et al., 2016)
5	1.8%Au/Al_2O_3, 1.2 mg mL^{-1}	22	1110	H_2O_2, 2.2 equiv.	120	10	NC	12900	83	87	72.2	(Rautiainen et al., 2016)

1179a: metal loading is weight ratio; b: metal loading detected by ICP-OES; c: 1 equiv. NaOH added initially; d: selectivity to GOA; e: yield of GOA

1180TOF: turnover frequency; NC: not controlled; — : not available or not applicable; * calculated based on equation: yield (%) = conversion (%) × selectivity (%) /100

1181

Table 5 Photocatalytic oxidation of glucose

entry	Operating conditions							Catalytic efficiency				Ref.
	Catalyst [a] and dosage	Initial glucose concentration	Light source	Oxidant and dosage	Temperature /°C	Time/ min	pH and reagent	TOF/h^{-1}	Conversion/%	Selectivity [i]/%	Yield [k]/ %	
1	TiO_2 [b], 1 g L^{-1}	2.8 mmol L^{-1} [d]	mercury lamp (λ_{max} = 365 nm), 125W	atmosphere	30	10	NC	—	11.0	71.3 [j]	7.8 *	(Colmenares et al., 2011)
2	TiO_2 [c], 1 g L^{-1}	1 g L^{-1} [d]	mercury lamp (λ_{max} = 365 nm), 400W	—	—	30	NC	—	69.5	~ 8.6 *	~ 6	(Payormhorm et al., 2017)
3	3%Au/TiO_2, 25 mg mL^{-1}	100 mmol L^{-1}	UV light (λ=350–400 nm), 0.3 W cm^{-2}	—	30	240	— [f], Na_2CO_3	—	> 99	> 94.9 *	94	(Zhou et al., 2017)
4	3%Au/TiO_2, 25 mg mL^{-1}	100 mmol L^{-1}	Visible light (λ=350–400 nm), 0.3 W cm^{-2}	—	30	240	— [f], Na_2CO_3	—	> 99	~ 100.0 *	99	(Zhou et al., 2017)
5	0.68%Au/TiO_2, 0.5 mg mL^{-1}	50 mg mL^{-1}	Standard photovoltaic air mass 1.5G conditions (0.1 W cm^{-2})	H_2O_2, 1.1 equiv.	Room temperature	10	— [g], NaOH	—	49	< 81	< 39.7 *	(Omri et al., 2018)
6	0.40%Au/Al_2O_3, 0.5 mg mL^{-1}	50 mg mL^{-1}	Standard photovoltaic air mass 1.5G conditions (0.1 W cm^{-2})	H_2O_2, 1.1 equiv.	Room temperature	10	— [g], NaOH	—	69	> 95	> 65.6 *	(Omri et al., 2018)
7	0.50%Au/CeO_2, 0.5 mg mL^{-1}	50 mg mL^{-1}	Standard photovoltaic air mass 1.5G conditions (0.1 W cm^{-2})	H_2O_2, 1.1 equiv.	Room temperature	10	— [g], NaOH	752380 [h]	> 99	> 95	> 94.1 *	(Omri et al., 2018)
8	1.1%Au/CeO_2, 0.5 mg mL^{-1}	50 mg mL^{-1}	Standard photovoltaic air mass 1.5G conditions (0.1 W cm^{-2})	O_2, atmosphere	NC [e]	270	— [g], NaOH	—	96	94	90.2 *	(Golonu et al., 2020)
9	ZnO/$CoPzS_8$(0.5%), 0.4 mg mL^{-1}	8 mmol L^{-1}	Simulated sunlight, 1.5 W cm^{-2}	air, 20 mL min^{-1}	Room temperature	300	NC	—	75	~ 10	~ 7.5 *	(Cheng et al., 2019)
10	SnO_2/ $FePz(SBu)_8$(0.1%), 0.4 mg mL^{-1}	1 mmol L^{-1}	Simulated sunlight, 2 W cm^{-2}	air, 400 mL min^{-1}	Room temperature	180	NC	—	34.2	32.9	11.3 *	(Zhang et al., 2019)
11	TiO_2/HPW(29%)/ CoPz(1%), 1 mg mL^{-1}	5 mmol L^{-1}	Simulated sunlight, 1.70 W cm^{-2}	ambient air	Room temperature	180	NC	—	22.2	63.5	14.1 *	(Yin et al., 2020)
12	g-C_3N_4/CoPz(0.5%), 0.67 mg mL^{-1}	1 mmol L^{-1}	Simulated sunlight, 2 W cm^{-2}	H_2O_2, 30%, 30 μL	Room temperature	20	NC	—	52.1	~ 60	~ 31.3 *	(Zhang et al., 2020)

1183a: loading is weight ratio; b: prepared under ultrasound; c: powders prepared under ultrasound with assistance of CTAB; d: solvent was mixture of Milli-Q water and 1184acetonitrile (10/90, v/v); e: increased to ~ 39 °C; f: 0.1 mol L^{-1} Na_2CO_3 added initially; g: 1 equiv. NaOH added initially; h: calculated by the conversion at 15 min; i: 1185selectivity to GOA; j: total selectivity to GAA, GOA, and arabitol; k: yield of GOA

1186TOF: turnover frequency; Pz: thioporphyrazine; HPW: phosphotungstic acid; NC: not controlled; — : not available or not applicable; * calculated based on equation:
1187yield (%) = conversion (%) × selectivity (%) /100

1188

Table 6 Strengths and limitations (denoted by the symbols ✓ and ×, respectively) of existing catalytic technologies for glucose oxidation to GOA/GAA.

Method	**Catalyst**		
	Monometal	Bimetal	Bifunction/composite
Conventional heating	✓ High selectivity × Pressured oxygen required	✓ High selectivity × High temperature or long time required	✓ Direct conversion of di- and polysaccharides × High temperature required
Ultrasound	✓ Adjustable selectivity ✓ High yield ✓ Power saving × Atmosphere required	—	—
Microwave	✓ High efficiency × Relatively strong oxidant required	—	—
Photochemistry	✓ High conversion and selectivity × Base required	—	✓ No base required × Low conversion and complex product profile
Electrochemistry	✓ Good selectivity ✓ Simultaneous production of H_2 × Strict requirement of complex set-ups × Strong base required		

— : not reported in the literature to the best of our knowledge